The role of Peptidylarginine deiminase 4 (PAD4) and Endothelial–Mesenchymal Transition (EndMT) in pancreas-heart axis of Type 1 diabetes mellitus

Hsu Lin Kang

PhD Dissertation

Szeged
2026.

Doctoral School of Experimental and Preventive Medicine
Albert Szent-Györgyi Medical School
University of Szeged

The role of Peptidylarginine deiminase 4 (PAD4) and Endothelial–Mesenchymal Transition (EndMT) in pancreas-heart axis of Type 1 diabetes mellitus

PhD Dissertation

Hsu Lin Kang

Supervisor:
Krisztina Kupai MD, PharmD, PhD

Szeged

1. Table of Contents

1. Table of Contents **3**

2. List of publications linked to the thesis **5**

3. Introduction **6**

3.1. Diabetes mellitus 6

3.2. Type 1 diabetes mellitus (T1DM) 6

3.3. Peptidylarginine deiminases (PADs) 7

3.4. Role of NETosis markers in diabetes (PAD4, Citrullinated Histone H3, Neutrophil Elastase) 8

3.5. Streptozotocin (STZ)-Induced Diabetic Rat 9

3.6. Expression of cytokines in β-cells injured by STZ through glucose transporter 2 (GLUT2) 10

3.7. Inflammation markers and PAD4 11

3.8. Diabetic heart and Endothelial-to-Mesenchymal Transition (EndMT) 13

3.9. Inducible Nitric Oxide Synthase (iNOS) and Myeloperoxidase (MPO) in Heart and Neutrophils 14

3.10. Peroxynitrite (ONOO-) interacts with matrix metalloproteinase(MMPs) and tissue inhibitors of MMPs (TIMPs) 15

3.11. The Role of Inflammation in Cardiac Fibrosis Complications 18

3.12. Cytokines and EndMT in Citrullinated Heart 19

3.13. Cl-amidine: a PADs inhibitor 20

4. Objectives **22**

5. Materials and Methods **23**

5.1. Experimental Protocol for studying PAD4 23

5.2. Measurement of Calcium Ion in the Pancreas in Exp. A 24

5.3. Western Blot of CITH3, PAD4 in Exp. A 24

5.4. Measurement of Pancreatic TNF-α, IFN-γ, IL-6, IL-10, IL-18, NETosis, and IL-33 Concentrations in Exp. A 25

5.5. RNA Extraction, Reverse Transcription, and Quantitative Real-Time Polymerase Chain Reaction (qRT-PCR) in Exp. A 25

5.6. STZ injection for EndMT study in Exp. C 26

5.7. Determination of Cardiac Cytokines ROS, EndMT Markers (IL 18,6,33,10, lL-β1, ROS, Peroxynitrite ($ONOO^-$), Nitric Oxide Synthases (NOS) Isoforms, and TNF-α Concentration in Exp. C 26

5.8. Matrix Metalloproteinase 2 (MMP-2), MMP-2 Zymography in Exp. C 27

5.9. Western Blot Analyses of Cardiac Discoidin Domain Tyrosine Kinase Receptor 2 (DDR-2),Citrullinated Histone H3 (H3Cit), Vimentin in Exp. C 27

5.10. Determination of Cardiac Myeloperoxidase (MPO) Activity in Exp. C 28

5.11. Protein Content Measurement from heart in Exp. C 28

5.12. Statistical Analysis 28

6. Results **29**

6.1. Verifying That STZ Injured the Pancreatic Tissue at the SIXTH Week in (Exp. A), PAD4 enhance group 29

6.2. Validating the Inflammation in Pancreas During the Sixth Week in (Exp. A) 29

6.3. PAD4 mRNA Level in the Pancreas at the Sixth Week in (Exp. A) 30

6.4. The Expression of PAD4 and Citrullinated Protein in the Pancreas at the Sixth Week in (Exp. A) 30

6.5. Ca^{2+}: A Prerequisite Cofactor for Citrullination Among PADs in the Sixth Week in (Exp. A) 31

6.6. Blood Glucose Measurement Before Termination in (Exp. A) and B 32

6.7. NETosis Level in the Serum and Pancreas in (Exp. B) 32

6.8. The Expression of Various Cytokines in the Heart 33

6.9. Basic ROS Examination in the Heart 34

6.10. Nitric Oxide Synthases (NOS) Determination in the Heart 34

6.11. The Assessment of EndMT by DDR-2, MMP-2, and TIMP-1 in the Heart 34

6.12. Biomarkers of Mesenchymal Cells and Neutrophils in the Heart 35

6.13. TGF-β Level of Heart, Aorta, and Plasma 36

6.14. Endothelin-1 Expression in Heart and Aorta 36

7 Discussion **37**

8. Summary **44**

9. Acknowlegements **45**

10. References **46**

2. List of publications linked to the thesis

MTMT identification: 10094398

1. **Kang, H. L.,** Szász, A., Valkusz, Z., Várkonyi, T., Pósa, A., & Kupai, K. (2025). **Targeting PAD4: A Promising Strategy to Combat β-Cell Loss in Type 1 Diabetes.** *International Journal of Molecular Sciences*, *26*(13), 6113. **IF:4.9, D/Q rank: Q1**

2. **Kang, H. L.,** Várkonyi, Á., Csonka, Á., Szász, A., Várkonyi, T., Pósa, A., & Kupai, K. (2025). **Endothelial–Mesenchymal Transition and Possible Role of Cytokines in Streptozotocin-Induced Diabetic Heart.** *Biomedicines*, *13*(5), 1148. **IF:3.9, D/Q rank: Q1**

Other publications:

3. Kupai, K., **Kang, H. L**., Pósa, A., Csonka, Á., Várkonyi, T., & Valkusz, Z. (2024). **Bone loss in diabetes mellitus: diaporosis.** *International Journal of Molecular Sciences*, *25*(13), 7269. **IF: 4.9, D/Q-rank: Q1**

4. Matusovits, D., Murlasits, Z., Kupai, K., Baráth, Z., **Kang, H. L.**, Osváth, P., ... & Pósa, A. (2023). **Paclitaxel Protects against Isoproterenol-Induced Damage in Rat Myocardium: Its Heme-Oxygenase Mediated Role in Cardiovascular Research**. *Antioxidants*, *12*(5), 1129. **IF: 6.6, D/Q-rank: Q1**

3. Introduction

3.1. Diabetes mellitus

Diabetes mellitus is a chronic, non-infectious metabolic disorder that primarily affects glucose metabolism, but also impacts protein and lipid metabolism. It is a major global contributor to mortality and morbidity. Current estimates suggest that more than 537 million people have diabetes worldwide, and this number is projected to increase over time. [1]. Diabetes is defined by hyperglycaemia, which is caused by relative or exact insulin insufficiency. [2]. Such meticulous control supports overall well-being and mitigates complications linked to both hyperglycemia and hypoglycemia. The regulation of glucose homeostasis relies on a complex interaction of hormones and neuropeptides produced by the pancreas, liver, brain, gut, adipose tissue, and muscle. These biochemical mediators collaboratively ensure effective blood sugar regulation and promote physiological balance. [3]. The endocrine pancreas is responsible for the secretion of two principal hormones, glucagon and insulin, both of which are essential for the regulation of blood glucose homeostasis.

3.2. Type 1 diabetes mellitus (T1DM)

Type 1 diabetes mellitus (T1DM) is a chronic autoimmune disorder defined by an absolute deficiency of insulin. This condition arises when the immune system erroneously targets and destroys the pancreatic beta cells responsible for insulin production. [4]. It makes up roughly 5–10% of all diabetes individuals. [2]. Polymorphisms in human leukocyte antigen (HLA) DR and HLA DQ are associated with an increased risk for developing T1DM. [5]. Class II HLA DR and DQ present antigens to helper T-cells with $CD4^+$ [6]. Studies have found that both genetic predisposition and environmental factors contribute to the development of T1DM by inducing stress in the endoplasmic reticulum of beta cells. [7]. Environmental factors consist of low vitamin D levels, limited sunlight exposure, maternal age above 35, certain viral infections (such as retroviruses, picornaviruses, enteroviruses, herpesviruses, and rotaviruses), and issues related to the gut microbiome. [4]. Glutamic acid decarboxylase 65 (GAD65), insulinoma antigen 2 (IA2), zinc transporter (ZnT8), non-specific islet cell autoantigens (ICA), pancreatic duodenal homeobox factor 1 (PDX1), chromogranin A (CHGA), islet-specific glucose-6-phosphatase catalytic subunit-related protein (IGRP), heat shock protein 60 (hsp60), and islet cell antigen 69 (ICA69) are considered to be the primary islet β-cell autoantigens for autoreactive T-cells.[4,8]. In T1DM, immune responses typically target autoantigens, leading to the destruction of beta cells. Current understanding suggests that pancreatic autoantigens are

processed by macrophages, dendritic cells, or B-lymphocytes functioning as antigen-presenting cells, and are then presented to naive T-cells in pancreatic lymph nodes, resulting in the generation of autoreactive CD4+ T-cells. However, the exact mechanisms underlying the initiation and progression of beta-cell loss remain unclear. Autoreactive T-cells secrete cytokines that stimulate CD8+ cytotoxic T-cells and promote B-lymphocyte, dendritic cell, and macrophage proliferation, ultimately causing beta-cell death [9].

3.3. Peptidylarginine deiminases (PADs)

Peptidylarginine deiminases (PADs) constitute a group of calcium-dependent enzymes that catalyze the post-translational conversion of arginine residues to citrulline, a process called citrullination or deimination. This modification changes protein structure and function, affecting gene regulation, immune responses, and cellular signaling. In humans, there are five PAD isoforms (PAD1, PAD2, PAD3, PAD4, and PAD6), each exhibiting tissue-specific expression. PAD2 and PAD4 have been studied for their involvement in the central nervous system and immune system. PAD2 is distributed across the brain, spinal cord, skeletal muscles, pancreas, and immune cells, while PAD4 is primarily found in granulocytes and monocytes. Both enzymes participate in regulating gene transcription via histone citrullination and are involved in processes such as NETosis and pyroptosis [10,11]. **(Figure 1.)**

Dysregulation of PAD activity has been observed in various pathological conditions. In the brain, PAD2 and PAD4 are present in the cerebral cortex and hippocampus, and their altered activation has been linked to neurodegenerative diseases, including Alzheimer's disease (AD). Increased citrullination of proteins in the central nervous system is associated with the development of protein aggregates and neuroinflammation, which are characteristic of AD pathology. In the immune system, PAD2 and PAD4 are involved in the pathogenesis of autoimmune diseases such as rheumatoid arthritis (RA) by generating citrullinated proteins that act as autoantigens and stimulate the production of anti-citrullinated protein antibodies (ACPAs), a marker of RA. PAD2 also contributes to macrophage differentiation and immune signaling, indicating its involvement in both physiological and disease processes. Research on PAD inhibitors is ongoing to assess their therapeutic potential in inflammatory and neurodegenerative disorders [12,13].

Figure 1. The diagram briefly depicts the five primary human PAD enzymes.

3.4. Role of NETosis markers in diabetes (PAD4, Citrullinated Histone H3, Neutrophil Elastase)

In T1DM, the formation of neutrophil extracellular traps (NETs) has been identified as a significant factor contributing to pancreatic inflammation and β-cell destruction. The process of NETosis is mediated by the enzyme peptidylarginine deiminase 4 (PAD4), which facilitates the citrullination of histone H3 (CITH3). This modification leads to chromatin decondensation and the subsequent release of DNA-protein complexes known as NETs. Notably, pharmacological inhibition of PAD4 using Cl-amidine considerably reduced NETosis and inflammation, emphasizing the pivotal role of PAD4 in T1DM pathogenesis and its promise as a therapeutic target [14–16].

Additional data from both human and murine models further corroborate the association between hyperglycemia and enhanced NETosis. Neutrophils isolated from individuals with T1DM display increased PAD4 expression and an augmented propensity for NET formation upon exposure to elevated glucose conditions. Raised levels of CITH3 and neutrophil elastase

(NE) are observed in diabetic wound tissues and blood samples, reflecting systemic NETosis activity. Importantly, PAD4-deficient mice exhibit reduced NET generation and improved wound healing, highlighting the enzyme's involvement in diabetes-associated tissue injury. Mechanistically, calcium influx activates PAD4, leading to histone citrullination and chromatin release, while NE further degrades nuclear components, thereby intensifying NETosis. Collectively, these findings indicate that NETosis markers—PAD4, CITH3, and elastase—serve not only as biomarkers of inflammation but also as active mediators of autoimmune and inflammatory damage in T1DM. (**Figure 2.)**

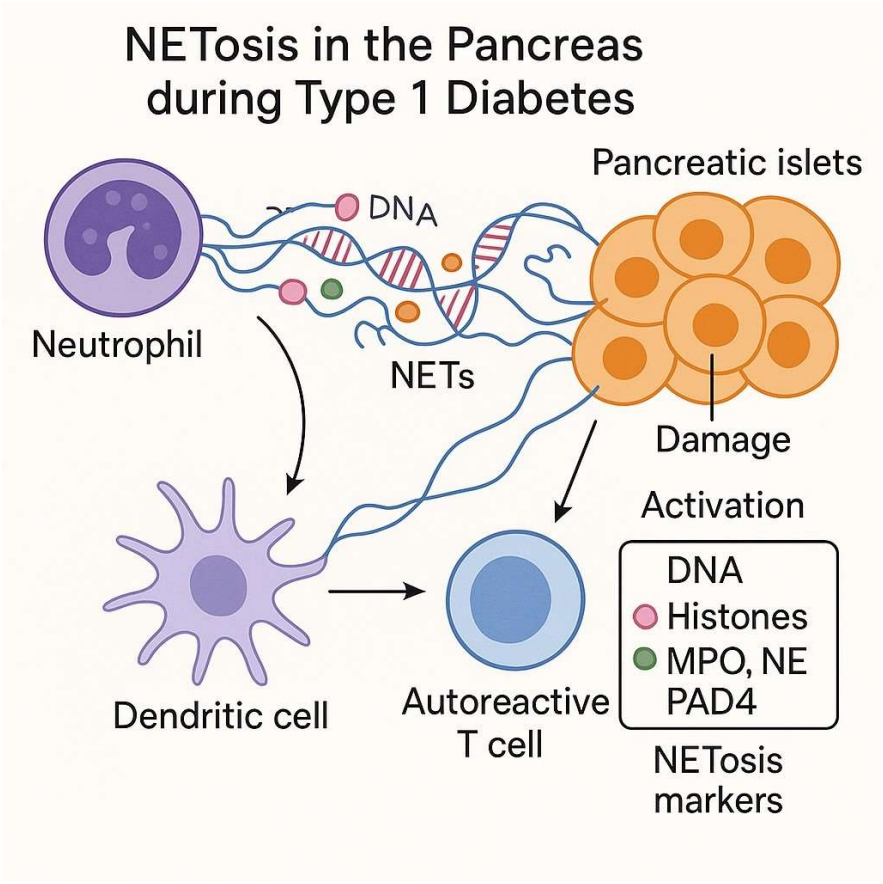

Figure 2. A schematic diagram illustrating NETosis in the pancreas during T1DM.

It highlights how neutrophils release NETs that infiltrate pancreatic islets, damage beta cells, and activate immune responses. MPO, myeloperoxidase ; CITH3, Histone H3 citrullination ; NE, neutrophil elastase.

3.5. Streptozotocin (STZ)-Induced Diabetic Rat

Streptozotocin (STZ) is an antibiotic that destroys pancreatic islet β-cells. It is commonly used in experiments to create a model of T1DM. The diabetogenic characteristics of STZ, which was first discovered from *Streptomyces achromogenes* in 1960, were not disclosed until 1963 [17].

Junod, Lambert, Stauffacher, and Renold (1969) defined this activity based on earlier studies [18] showing that the diabetogenic effects are caused by the selective death of pancreatic islet β-cells.This activity causes the rats to exhibit symptoms of T1DM [19], including insulin insufficiency, hyperglycemia, polydipsia, and polyuria. Males are more susceptible to STZ than females, and age has an inverse relationship with susceptibility to the diabetogenic effects of STZ. Interestingly, some rat strains, such as Wistar-Kyoto rats, exhibit resistance to STZ, whereas the more common strains, Wistar and Sprague-Dawley rats, do not. The major methods of administering STZ are intraperitoneal (IP) and intravenous (IV).

Rats and mice are the predominant species used in diabetic research, accounting for a remarkable 94% of the field's publications [20]. This preference is largely attributed to their rapid reproduction rates, short generation intervals, and ease of accessibility, making them invaluable in endocrinology research [21,22]. Their widespread use has significantly advanced our understanding of diabetes and its underlying mechanisms. The ability of STZ-injection to modify the disease makes the rat model of diabetes highly comparable to human conditions [23]. Rats are favored in diabetes research due to their short gestation period of 21–22 days and their sexual maturity reached at postnatal days 60–70 [24,25]. These characteristics make them ideal for studying the effects of various treatments on disease progression and management. Furthermore, their physiological responses to diabetes are remarkably similar to those observed in humans, providing valuable insights into the effectiveness and safety of potential therapies.

Chemically induced models of T1DM in rats often involve the administration of STZ in varying doses and methods. Researchers may use a single high dose of STZ, ranging from 35 to 65 mg/kg, administered either IV or IP, as noted by Srinivasan and Ramarao in 2007 [22].

3.6. Expression of cytokines in β-cells injured by STZ through glucose transporter 2 (GLUT2)

Through GLUT2, STZ, a cytotoxic glucose analog, tends to accumulate in pancreatic beta cells. Based on the structure of the bond between the carbon-2 of hexose and N-methyl-N-nitrosourea (MNU), STZ operates as an analogue of nitrosourea. The methyl-nitrosourea moiety of STZ's DNA alkylating activity determines how hazardous it is. DNA fragmentation results from the methyl group being transferred from STZ to the DNA molecule, which damages the molecule in a specific sequence of events [26]. (**Figure 3.**)

While GLUT2 is also expressed in smaller amounts in the small intestine, kidneys, and central nervous system, it serves as the primary glucose transporter in the β-cells of pancreatic islets and hepatocytes. Under typical conditions, GLUT2 facilitates the movement of glucose into cells, allowing for the equalization of glucose concentrations on both sides of the cell membrane. Importantly, variations in GLUT2 have been linked to a range of metabolic and endocrine disorders, highlighting its critical role in maintaining normal physiological functions. In addition to direct cytotoxicity, STZ also triggers oxidative stress and inflammatory responses, further exacerbating beta-cell damage [26]. The loss of beta cells initiates a cascade of immune responses, including the activation of resident macrophages and infiltration of immune cells into the islets [27].

Cytokines play a pivotal role in mediating and amplifying the inflammatory response during STZ-induced beta-cell destruction. Proinflammatory cytokines such as interleukin-1β (IL-1β), interferon-γ (IFN-γ), and tumor necrosis factor-α (TNF-α) are upregulated and contribute to beta-cell dysfunction by activating nuclear factor-kappa B (NF-κB) signaling pathways, leading to increased expression of inducible nitric oxide synthase (iNOS) and nitric oxide production, which are toxic to beta cells. Interestingly, several investigations have demonstrated that during beta-cell death, neutrophils might infiltrate the pancreas due to the attraction of cytokines and chemokines [28].

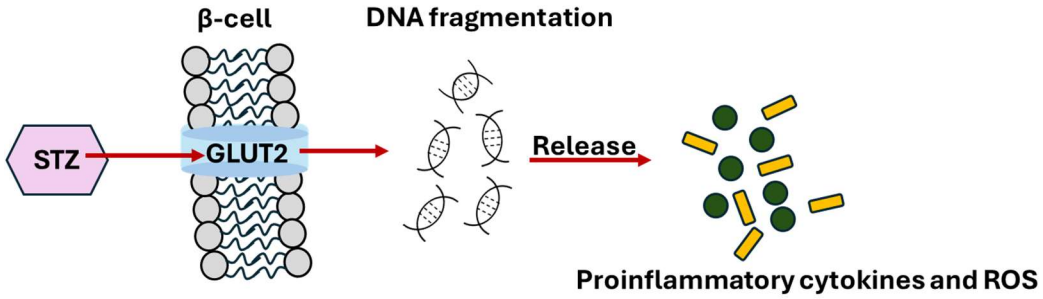

Figure 3. The STZ pathway in the pancreas

3.7. Inflammation markers and PAD4

Cytokines and chemokines are key regulators of PAD4 activity in neutrophils, initiating the process of NETosis. PAD4 catalyzes the citrullination of histone proteins—particularly histone H3—resulting in chromatin decondensation, which is essential for NET formation. Pro-inflammatory cytokines such as TNF-α and IL-8, together with chemokines including CXCL-1 and CXCL-2, activate neutrophils via G-protein–coupled receptors and subsequent intracellular signaling pathways involving PKC, Raf-MEK-ERK, and NADPH oxidase. These

cascades facilitate the production of reactive oxygen species (ROS), further enhancing PAD4 activation. Once activated, PAD4-mediated histone citrullination relaxes chromatin structure, allowing the release of DNA decorated with antimicrobial proteins such as elastase and myeloperoxidase (MPO), thus forming NETs [29].

Persistent inflammatory stimuli or unresolved infections can intensify PAD4-driven NETosis. Inchronic inflammatory conditions, prolonged exposure of neutrophils to cytokines and chemokines leads to sustained PAD4 activation and excessive NET generation, which may cause tissue injury and contribute to the development of autoimmune and thrombo-inflammatory disorders. Notably, TNF-α not only stimulates PAD4 but also enhances IL-8 production, serving as a strong chemoattractant and activator for neutrophils. Elastase released during NETosis contributes to extracellular matrix degradation and propagates the inflammatory response. In pathologies such as rheumatoid arthritis and sepsis, elevated concentrations of citrullinated histones and elastase act as biomarkers for NETosis and correlate with disease severity [30]. (**Figure 4.)**

Further, PAD4's activity is not limited to histone citrullination; it also modifies other substrates such as glycogen synthase kinase-3β and ADAMTS13, thereby affecting broader immunological and coagulation mechanisms. The regulation of PAD4 depends on calcium influx and may be influenced by post-translational modifications or protein interactions that lower its calcium threshold. Biomarkers like MPO, NE, and CITH3 are consistently upregulated in PAD4-mediated NETosis, offering reliable indicators of neutrophil activation and systemic inflammation. Elucidating these molecular mechanisms provides potential therapeutic targets aimed at modulating PAD4 activity to address NET-related diseases while maintaining host immune competence [31].

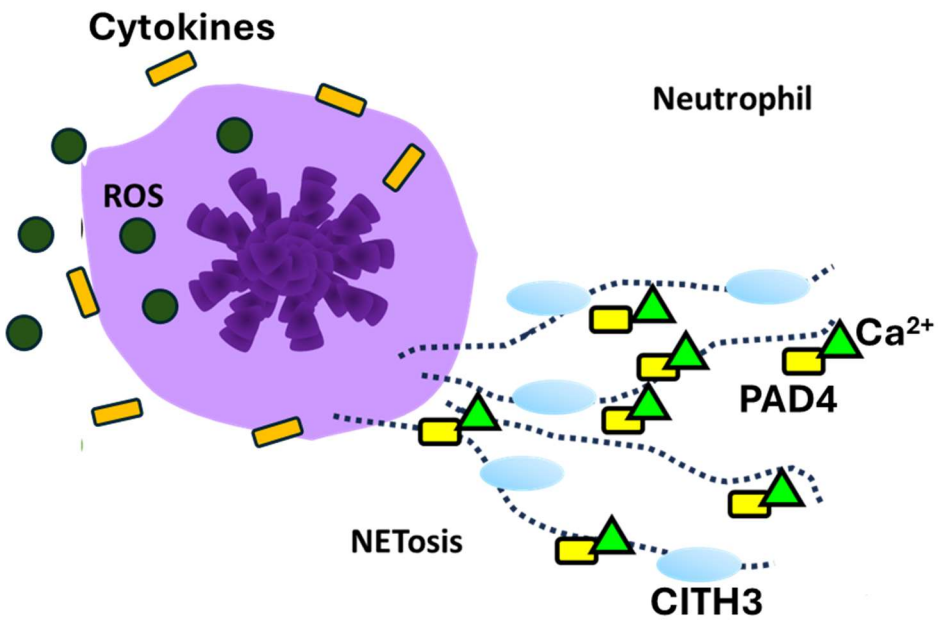

Figure 4. The diagram illustrates NETosis.

A variety of ROS and cytokines may stimulate NETosis. CITH3, Histone H3 citrullination

3.8. Diabetic heart and Endothelial-to-Mesenchymal Transition (EndMT)

DM is a leading global health burden and a major risk factor for cardiovascular disease (CVD) [32]. (**Figure 5.)** Despite intensive glucose-lowering strategies, patients with diabetes continue to experience elevated cardiovascular morbidity and mortality, pointing to underlying mechanisms beyond hyperglycemia alone [33]. A growing body of evidence identifies endothelial-to-mesenchymal transition (EndMT) as a crucial pathophysiological process linking diabetes to cardiac dysfunction and vascular complications [34]. EndMT refers to the transdifferentiation of endothelial cells (ECs) into mesenchymal-like cells. During this transition, ECs lose their characteristic markers, such as VE–cadherin and CD31, and acquire mesenchymal features, including α-SMA and collagen I. This shift promotes extracellular matrix (ECM) deposition, fibrosis, and vascular stiffness [35]. In the diabetic context, hyperglycemia, oxidative stress, and chronic inflammation act synergistically to drive EndMT both locally and systemically. In vitro studies using human umbilical vein endothelial cells (HUVECs) show that high glucose environments induce EndMT through the TGF-β1/ ERK pathway. Suppression of this transition has been achieved with ERK inhibitors like PD98059 or antioxidants such as N-acetylcysteine [36]. Consistent with these findings, cardiac tissues from diabetic patients display increased mesenchymal marker expression, indicating persistent EndMT even under controlled glycemia [37].

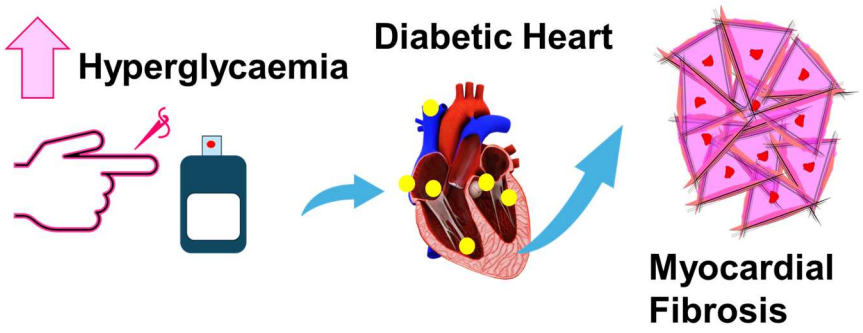

Figure 5. The clinical background to cardiovascular disease in diabetic patients.

3.9. Inducible Nitric Oxide Synthase (iNOS) and Myeloperoxidase (MPO) in Heart and Neutrophils

Inducible nitric oxide synthase (iNOS) and myeloperoxidase (MPO) are critical enzymes in neutrophils that govern inflammatory responses and contribute to the generation of NETs, a process highly reliant on PAD4. PAD4 mediates histone citrullination, which facilitates chromatin decondensation and subsequent NET release. MPO, contained within azurophilic granules, not only produces reactive oxidants such as HOCl but also regulates neutrophil activation, lifespan, and NET formation [15]. iNOS, through the production of nitric oxide (NO), modulates oxidative stress and inflammatory signaling pathways, indirectly influencing PAD4 activity and NETosis. In cardiovascular disease, especially following myocardial infarction (MI), PAD4-dependent NETs have demonstrated roles in shaping macrophage polarization toward an anti-inflammatory M2 phenotype, thus promoting tissue repair. Conversely, PAD4 deficiency is associated with heightened inflammation, impaired healing, and altered cardiac remodeling [38].

Within the context of heart failure and chronic cardiac inflammation, NETosis—mediated by PAD4, MPO, and NE—drives processes such as myocardial fibrosis, cardiomyocyte death, and adverse remodeling. These mechanisms are integral to heart failure progression. Although NETs initially serve protective functions, their dysregulation can result in persistent inflammation and tissue injury. The citrullination of histones by PAD4 is pivotal for NET formation, and excessive PAD4 activity has been implicated in autoimmune and thrombo-inflammatory disorders. MPO further intensifies this response by promoting chromatin decondensation and facilitating NET release. Collectively, these enzymes create a feedback loop that perpetuates neutrophil activation and inflammatory signaling within the cardiac environment, thereby exacerbating pathological progression [39].

EndMT involves the loss of endothelial characteristics and the acquisition of mesenchymal features, contributing to fibrosis and vascular dysfunction in cardiovascular pathology. Chronic inflammation and oxidative stress—conditions augmented by NETs and their constituents such as MPO and PAD4—are potent drivers of EndMT [40]. NETs compromise endothelial integrity, enhance TGF-β signaling, and facilitate the conversion of endothelial cells into myofibroblast-like phenotypes, establishing a mechanistic link between neutrophil activity and EndMT. This association underscores the roles of iNOS, MPO, and PAD4 not only in immune regulation but also in vascular remodeling and fibrosis via EndMT, highlighting their potential as therapeutic targets in the management of heart disease [41]. (**Figure 6.)**

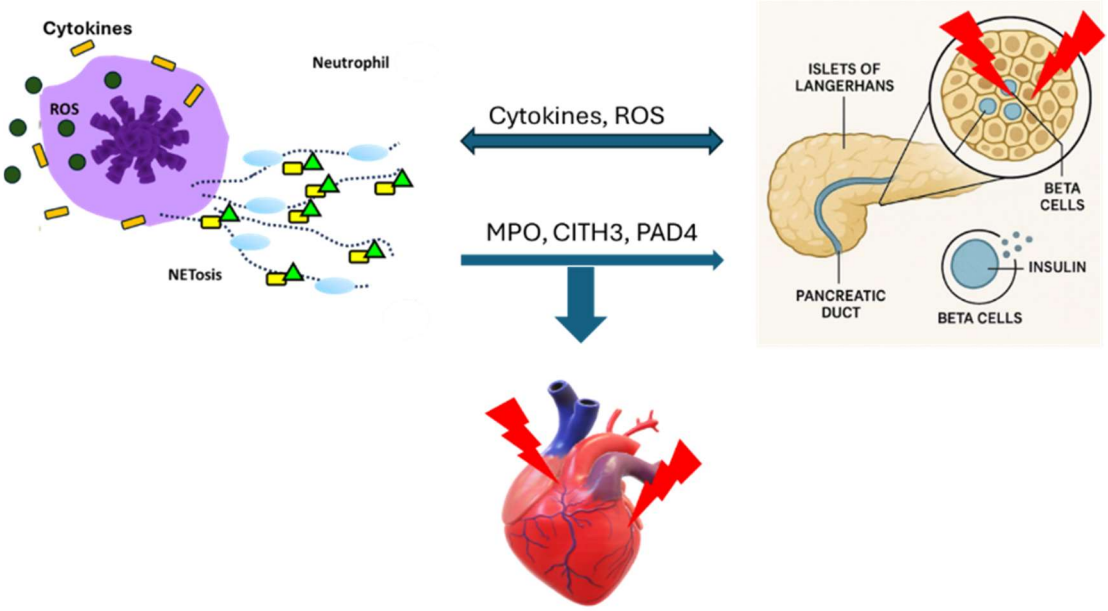

Figure 6. The role of neutrophil and inflammatory mediators media in the pancreas-heart axis

3.10. Peroxynitrite (ONOO-) interacts with matrix metalloproteinase(MMPs) and tissue inhibitors of MMPs (TIMPs)

Peroxynitrite ($ONOO^-$), a reactive nitrogen species generated through the reaction of nitric oxide (NO) with superoxide (O_2^-), plays a critical role in mediating oxidative stress and inflammation within cardiovascular diseases [38]. In neutrophils, peroxynitrite is capable of activating PAD4, thereby enhancing histone citrullination and facilitating the formation of NETs. This mechanism contributes to endothelial dysfunction and myocardial injury. In the context of heart disease, increased levels of peroxynitrite aggravate tissue injury by modifying proteins, lipids, and DNA, as well as perpetuating inflammatory signaling pathways. Activation of PAD4 by peroxynitrite serves as a mechanistic link between oxidative stress, chromatin remodeling, and NETosis, processes implicated in both acute and chronic cardiac pathologies.

Matrix metalloproteinases (MMPs) and their endogenous inhibitors, tissue inhibitors of metalloproteinases (TIMPs), are essential for regulating extracellular matrix (ECM) remodeling in the myocardium. An imbalance in MMP/TIMP activity is associated with fibrosis, persistent inflammation, and structural changes in heart failure [42]. MMPs may indirectly modulate PAD4 function by shaping the inflammatory microenvironment and promoting neutrophil infiltration; for instance, elevated MMP-2 levels are linked to increased NET formation and PAD4 activation [43]. Conversely, TIMPs—particularly TIMP-1—can mitigate these pathological effects by restricting MMP activity and curbing neutrophil-mediated tissue injury [44]. The interaction among MMPs, TIMPs, and PAD4 underscores a complex regulatory system governing ECM composition, immune cell dynamics, and cardiac structural remodeling [45]. EndMT represents a pathological process that contributes to cardiac fibrosis and vascular dysfunction. NETs, under the influence of PAD4 and modulated by peroxynitrite and MMPs, can induce EndMT by disrupting endothelial junctions and activating profibrotic signaling pathways, including TGF-β and NF-κB. Peroxynitrite intensifies oxidative stress, a recognized inducer of EndMT, while MMPs facilitate endothelial cell detachment and transition by degrading basement membranes. PAD4-dependent NET formation further amplifies this progression via the release of inflammatory mediators and proteases. Collectively, the actions of peroxynitrite, MMPs, TIMPs, and PAD4 establish a pro-EndMT milieu, thus linking immune responses to fibrotic remodeling in cardiac disease [46]. (**Figure 7.)**

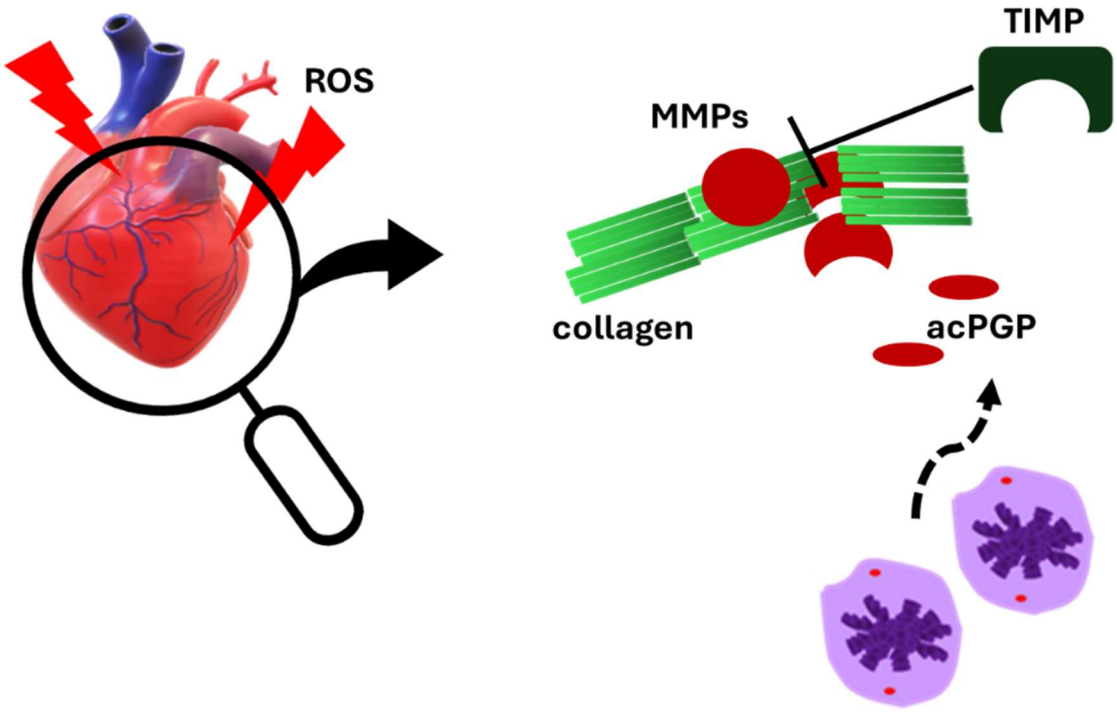

acPGP, or N-acetyl-proline-glycine-proline, is a matrikine derived from collagen breakdown by MMPs and directly attracts and activates neutrophils, causing calcium mobilization and the release of pro-inflammatory mediators

Figure 7. The diagram illustrating how MMPs, TIMPs and neutrophils are related in cardiac disorders. MMPs, Matrix Metalloproteinases; TIMPs, Tissue Inhibitors of Metalloproteinases; acPGP, N-acetyl-proline-glycine-proline.

3.11. The Role of Inflammation in Cardiac Fibrosis Complications

Cytokines and chemokines function as key mediators in both inflammation and fibrosis associated with cardiac pathologies, particularly through their regulatory effects on EndMT [47]. Transforming growth factor-beta (TGF-β) serves as a principal regulator of EndMT and fibrotic pathways, activating SMAD-dependent and independent mechanisms that prompt endothelial cells to relinquish markers such as VE-cadherin in favour of acquiring mesenchymal characteristics, including α-smooth muscle actin (α-SMA) and vimentin [48]. This cellular transition facilitates the proliferation of myofibroblasts, which are responsible for increased synthesis of extracellular matrix proteins like collagen, ultimately resulting in cardiac tissue stiffening and scarring. Pro-inflammatory cytokines, such as IL-1β and TNF-α, can collaborate with TGF-β to intensify EndMT processes and fibrogenic activity [49].

In addition, chemokines such as CXCL-1 and CCL-2 significantly contribute to the recruitment of immune cells into cardiac tissue, perpetuating chronic inflammation and further enhancing EndMT [50,51]. These molecules also drive the generation of ROS, which activate TGF-β signalling and PAD4-mediated NETosis [52]. ROS exacerbate damage to endothelial cells while simultaneously reinforcing the transition to a mesenchymal phenotype. Increased expression of α-SMA and vimentin in endothelial cells undergoing EndMT is indicative of their conversion into cells with fibrogenic potential. Such mechanisms are especially pertinent in cases of heart failure and post-myocardial infarction, where ongoing inflammation and oxidative stress foster progressive cardiac fibrosis [53].

The complex interactions among cytokines, chemokines, ROS, and EndMT indicators, including α-SMA and vimentin, establish a sustained cycle of inflammation and fibrosis within cardiac tissue. TGF-β remains central in this network, integrating signals from oxidative stress and immune mediators to promote EndMT. The resultant mesenchymal cells contribute substantially to extracellular matrix accumulation and tissue rigidity, which are defining features of cardiac fibrosis. Therapeutic approaches targeting these molecular pathways—particularly those involving TGF-β signalling and ROS production—show promise in mitigating or reversing fibrotic cardiac remodelling [54].

3.12. Cytokines and EndMT in Citrullinated Heart

Cytokines are integral to the regulation of cardiac function, playing pivotal roles under both normal and pathological conditions. These small proteins, including TNF-α, TGF-β, and various interleukins (IL-1, IL-6, IL-8) [55], are central to inflammatory responses that can lead to heart diseases such as ischemic heart disease, myocardial infarction, and heart failure. In the realm of heart disease, cytokines serve as markers of inflammation and contribute directly to the pathogenesis of ischemic injury, positioning them as potential targets for therapeutic interventions [56]. Conversely, some cytokines are involved in tissue repair following ischemia, underscoring their dual role in both damaging and healing cardiac tissues [57].

In addition to cytokines, ROSs are crucial for heart health, acting as subcellular messengers within signal transduction pathways [58]. While low levels of ROS are vital for normal cellular functions, excessive ROS production results in oxidative stress, which is implicated in various cardiovascular diseases, including myocardial infarction and heart failure. EndMT is another significant process, wherein endothelial cells transform into mesenchymal-like cells, contributing to cardiac fibrosis and other cardiovascular pathologies [59].

Moreover, citrullination has been identified in heart failure patients, affecting the function of myofilament proteins and potentially linking inflammation to structural changes in the heart [60]. This modification can alter protein function and contribute to the progression of heart failure [61]. Understanding these complex interactions and modifications is essential for developing targeted therapies that address both the inflammatory and reparative processes within cardiac tissues, ultimately improving heart disease outcomes and patient health [62]. (**Figure 8.**)

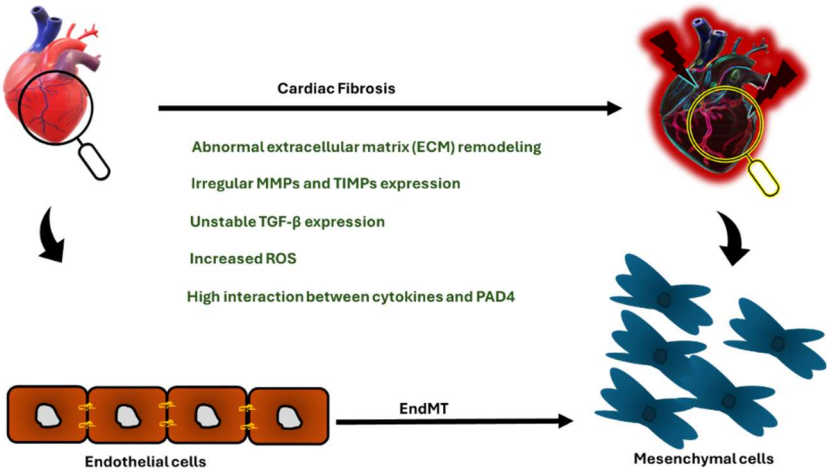

Figure 8. The brief mechanism of EndMT during cardiac fibrosis

3.13. Cl-amidine: a PADs inhibitor

Cl-amidine is an inhibitor of PADs, with a specific focus on targeting the PAD1, PAD3, and PAD4 enzymes. This compound demonstrates inhibitory concentration (IC50) values of 0.8 μM for PAD1, 6.2 μM for PAD3, and 5.9 μM for PAD4. By effectively inhibiting these enzymes, Cl-amidine plays a critical role in regulating the activity of PAD enzymes. This compound is well-regarded for its ability to induce apoptosis in cancer cells and arrest the cell cycle by upregulating the expression of microRNA-16. Furthermore, Cl-amidine inhibits histone 3 citrullination and the formation of neutrophil extracellular traps, both of which are critical processes in inflammatory responses. **(Figure 9.)** Its demonstrated effectiveness in enhancing survival rates in murine sepsis models underscores its significant potential for therapeutic applications. Additionally, ongoing research continues to uncover new dimensions of its efficacy, making it a promising candidate for further clinical exploration in various medical contexts [63].

This inhibition is particularly significant in diseases marked by excessive NETosis, such as rheumatoid arthritis, sepsis, and acute respiratory distress syndrome (ARDS). Research has demonstrated that localized delivery of Cl-amidine can effectively attenuate PAD4-mediated NETosis in tissue environments, presenting a targeted strategy to mitigate inflammation and tissue damage [64]. The intricate interplay between ROS, cytokines, and PAD4 highlights the complexity of immune regulation and the therapeutic potential of PAD4 inhibitors like Cl-amidine in managing inflammatory and autoimmune diseases [65,66].

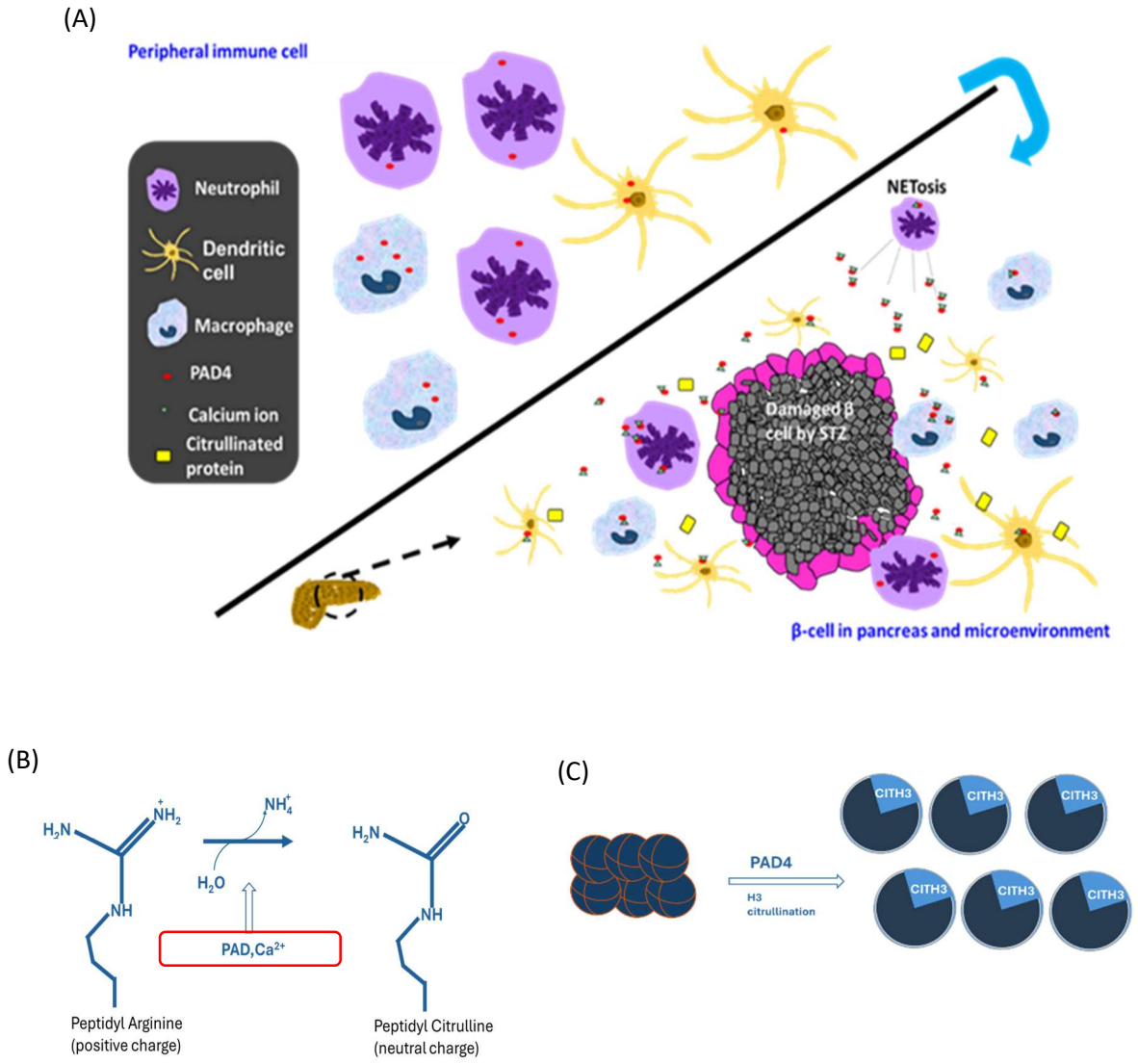

Figure 9. Diagram shows concept of STZ-induced NETosis in pancreas and citrullination. (A) Peripheral neutrophils infiltrate to pancreas during STZ-induced diabetes in pancreas (B) Ca^{2+} is a cofactor for activating PADs. (C) The process of NETosis is mediated by PADs, which facilitates the CITH3. This modification leads to chromatin decondensation and the subsequent release of DNA-protein complexes known as NETs.

4. Objectives/Aims

I. Investigate whether **PAD4-mediated histone citrullination and NETosis** represent a central, unifying mechanism in the pathogenesis of type 1 diabetes mellitus (T1DM).

II. Assess how increased **PAD4 activity in the pancreas** contributes to systemic inflammation.

III. Explore whether the resulting **proinflammatory** and **oxidative milieu** facilitates **endothelial–mesenchymal transition (EndMT)** in the diabetic heart.

IV. Integrate pancreatic and cardiac endpoints to establish PAD4 as a **common upstream driver of multi-organ diabetic complications**.

V. Provide a mechanistic rationale for the development of **PAD4-targeted therapeutic strategies**.

5. Materials and Methods

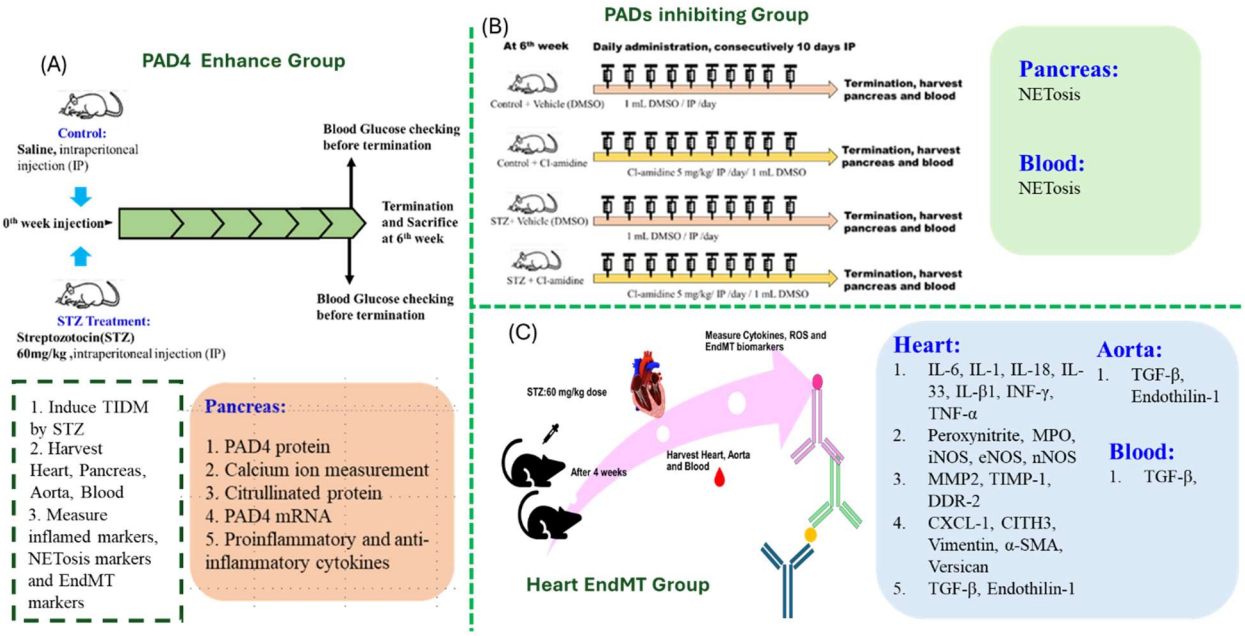

Figure 10. The summary of all experiments in current study. (A) In the A experiment, PAD4 enhance group, we employed STZ to promote PAD4 expression in the pancreas. Additionally, we investigated cytokines, Ca^{2+} levels, citrullinated histone 3, PAD4 mRNA, and protein (B) In the B experiment, PADs inhibiting group, we utilized Cl-amidine to inhibit PAD4. Next, we harvested pancreas and blood to determine the degree of NETosis. (C) In the C experiment, heart EndMT group, we used numerous markers to screen the heart, aorta, and blood during the EndMT mechanism.

5.1. Experimental Protocol for studying PAD4

After acclimation, Wistar Rats were able to discriminate between the T1DM group and the control group. The T1DM group received an intraperitoneal (IP) injection of streptozotocin (STZ) at a dose of 60 mg/kg/body weight (dissolved in saline), while the control group received an IP injection of saline in (Exp. A).(PAD4 enhance group) and B.(PADs inhibiting group). First, we performed experiment A to confirm PAD4 expression in STZ-induced diabetic rats (diabetes induced for 6 weeks). Second, we conducted a separate PAD4 inhibition trial ((Exp. B)) to evaluate the role of PAD4 in STZ-induced diabetic rats [67]. (Diabetes-induced duration with PAD4 inhibition: 6 weeks + 10 days of Cl-amidine I.P.)

In experiment B (PADs inhibiting group), we inhibited PAD4. The dose of Cl-amidine (Merck, 506282) was 5 mg/kg/IP for ten consecutive days. The vehicle for dissolving Cl-amidine was

dimethyl sulfoxide (DMSO, Merck, 102952), which was treated in the control group. Throughout the trial, each rat's weight was noted, and at the sixth week, it was euthanized. Before termination, each rat fasted for a day to allow for blood glucose measurements. Each rat's pancreas, blood, and liver were meticulously removed and used. Every tissue was stored in Triton at −80 °C for biological measurements.

5.2. Measurement of Calcium Ion in the Pancreas in (Exp. A)

The Calcium Detection Assay Kit (Abcam, ab102505, Waltham, MA, USA, range: 0.4–100 mg/dL) was used to measure the Ca^{2+} level after pancreas resection. All the pancreases were homogenized in PBS plus NP-40, then put on ice and centrifuged for five minutes at 10,000 rpm. The supernatants' measurements were carried out using the specified standards. Optical densities (ODs) were measured at $\lambda = 575$ nm. The data are expressed in nanograms per well.

5.3. Western Blot of CITH3, PAD4 in (Exp. A)

The pancreatic samples were stored in a solution that contained RIPA buffer (Merck Millipore, Burlington, MA, USA) and 1/10 of the final volume of phenylmethylsulfonyl fluoride (PMSF) (Sigma-Aldrich, Budapest, Hungary). Using the UP-100H Ultrasonic Homogenizer (Hielscher Ultrasonics, Teltow, Germany), the homogenates were homogenized three times for 10 s on ice before being centrifuged at 15,000× g for 10 min at 4 °C. The protein content of the supernatants was determined using the Bradford test. A total 50 μg of protein was extracted from each sample according to its protein content and placed onto 10% sodium dodecyl sulfate (SDS) polyacrylamide gels for two hours at a voltage of 90 V. The gels were transferred to nitrocellulose membranes after 2.5 h at 35 V. The membranes were dyed with Ponceau S and then washed with TBS-T (pH 7.4). The membranes were blocked in 5% BSA throughout the night. After blocking, blots were washed three times for 10 min in TBS-T. The first pair of antibodies—anti-PAD4 (Dilution: 1:3000, Catalog Number: 17373-1-AP, Proteintech, Manchester, UK) and anti-CITH3 (1:750, Catalog Number: ab5103, citrulline R2&R8&R17, Abcam, Cambridge, UK)— were incubated for two hours at room temperature. Then, using anti-mouse antibodies conjugated with horseradish peroxidase (DAKO Agilent, Santa Clara, CA, USA), they were kept for 1 h at room temperature. Quantity One Software version 4.5 (Bio-Rad Laboratories, Hercules, CA, USA) was utilized for analysis, and an enhanced chemiluminescence system (ECL Plus, Amersham Pharmacia Biotech., Buckinghamshire, UK) was used to display band pictures. Each membrane was stripped and used for the detection of β-actin for normalization (ab20272, Abcam, Cambridge, UK; anti-mouse secondary antibody,

DAKO Agilent, Santa Clara, CA, USA). The results were normalized to β-actin and presented as relative expressions.

5.4. Measurement of Pancreatic TNF-α, IFN-γ, IL-6, IL-10, IL-18, NETosis, and IL-33 Concentrations in (Exp. A)

After sacrifice, TNF-α (Invitrogen, Catalog: BMS622), IFN-γ (Invitrogen, Catalog: BMS621), IL-6, IL-10 (Invitrogen, Catalog: BMS625), IL-18 (Invitrogen, Catalog: KRC2341), NETosis (ELK Biotechnology, Catalog: ELK1521), and IL-33 (Abcam, Catalog: ab236714) levels were measured using ELISA kits obtained from several vendors and used in compliance with each manufacturer's recommendations.

5.5. RNA Extraction, Reverse Transcription, and Quantitative Real-Time Polymerase Chain Reaction (qRT-PCR) in (Exp. A)

Pancreatic samples were homogenized in 1 milliliter of TRIzol reagent (Life Technologies) using the MT-13K-L small, portable, homogenizer (MiuLab). Following the manufacturer's recommendations, the samples were centrifuged for 10 min at 13,000 rpm, and total RNA was isolated from the upper phase using the Monarch Total RNA Miniprep Kit (BioLabs). The quantity and quality of isolated RNA were evaluated using DeNovix DS-11 (DeNovix). The QuantiTect reverse transcription kit (Qiagen) was used to convert 100 ng of total RNA to cDNA in accordance with the manufacturer's instructions. cDNA levels were determined using QPCR and the Rotor-Gene Q real-time PCR System (Qiagen). The QuantiNova SYBR Green PCR Kit (Qiagen) was used to perform reactions using the following primer sets:

PAD4 sense: GCTCCCTCTCATCAGTTCCA.

PAD4 antisense: GGCTTGTCACTCGAGTTTTGA.

HPRT sense: CATTAATATTTAACGATGTGGATGCGTTTCA.

HPRT antisense: GCCTACCATCTTTAAACTGCACAAT.

In order to avoid false-positive results from the amplification of contaminated genomic DNA during the cDNA synthesis, we selected primers that had spanexon–exon junctions. There were at least four biological replicates used for each measurement. The ratio of each PAD4 mRNA to the HPRT was calculated using the $2^{-\Delta\Delta CT}$ technique [68]. (**Figure 11.**)

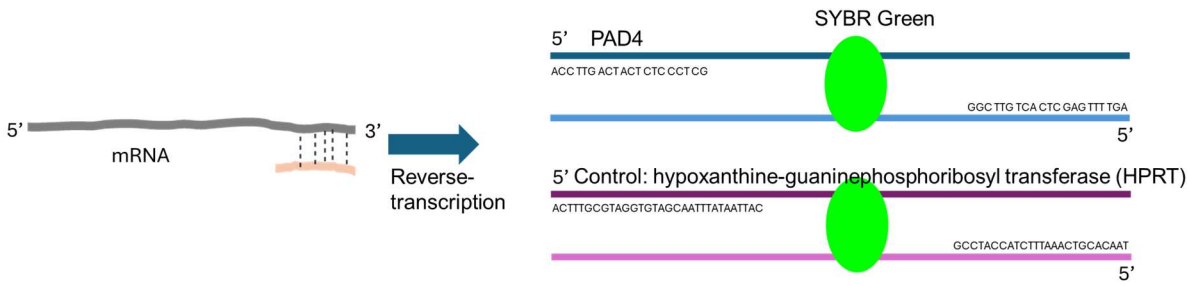

Figure 11. Scheme showing the primers and SYBR Green in RT-PCR

5.6. STZ injection for EndMT study in (Exp. C)

Male Wistar rats from BRC in Szeged, Hungary, were housed in cages as the experimental animals. Before they were sacrificed, the habitat was maintained for four weeks at a consistent temperature of 20–22 ◦C and humidity of 40–50% with a 12/12 h light/dark cycle. The rats weighed between 200 and 230 g, and they were fed and hydrated without restriction. Weighted measurements of body weight were taken both at the beginning and the end of this study. We just needed the bare minimum of rats to perform this experiment, and the required sample size was established using the resource equation and our prior trial as a guide (n = 5–15, depending on assay). We also piloted this trial in our laboratory. Every procedure was approved by the European Community rules and complied with the Directive of the European Parliament (2010/63EU). (Ethics license, University of Szeged: XXXIX./2040/2023). We were able to distinguish randomly between the Type 1 Diabetes Mellitus (T1DM) group and the control group following acclimatization. Intraperitoneal (IP) injections of saline were given to the control group, and 60 mg/kg/body weight of STZ was given to the T1DM group. Throughout the trial, the weight of each rat was noted, and, at the fourth week, they were all sacrificed. Each rat's heart and aorta were carefully removed and used. Blood samples were collected as well, for future measurements. Before analysis, every tissue was kept in −80 ◦C for biological measures.

5.7. Determination of Cardiac Cytokines ROS, EndMT Markers (IL 18,6,33,10, lL-β1, ROS, Peroxynitrite ($ONOO^-$), Nitric Oxide Synthases (NOS) Isoforms, and TNF-α Concentration in (Exp. C)

Cardiac samples were homogenized in ice-cold phosphate buffer (pH 7.4) for 20 s. After centrifugation (10 min, 3500 rpm, 4 ˚C), supernatants were collected carefully and used for ELISA and protein measurements. According to the manufacturer's datasheet (Gen Asia Biotech Co., Ltd., Shanghai, China), the amount of either 40 µL cardiac tissue supernatant or 50 µL standard solution was added to the wells that were pre-coated with cytokine/ROS

monoclonal antibody. Additionally, the supernatant-containing wells were completed with a second antibody labeled with biotin. Subsequently, Streptavidin-HRP was also added to both the supernatant and the standard-containing wells, which consequently formed an immune complex with a biotin-labeled antibody. After the incubation procedure at 37 ˚C, the plate was washed five times; thus, the unbound enzymes have been removed. For the color development, substrate solutions A and B were added to the wells and incubated for 10 min at 37 ˚C hidden from light. As the last step, the stop solution was pipetted, which resulted in a change from blue to yellow with the effect of acid. Theoptical density was measured at 450 nm. According to standard concentrations and the corresponding OD values, the linear regression equation of the standard curve and the samples' concentrations were calculated.

5.8. Matrix Metalloproteinase 2 (MMP-2), MMP-2 Zymography in (Exp. C)

The procedure for performing gelatin zymography was carried out as previously mentioned [69]. From rat heart homogenates, MMP-2 was extracted as follows: on an 8% SDS-polyacrylamide gel copolymerized with 2 mg/mL gelatin from pig skin, 50 µg protein/lane was loaded and separated by electrophoresis under non-reducing conditions (Sigma-Aldrich; St. Louis, MO, USA). Following electrophoresis, gels were gently shaken and cleaned in 2.5% Triton-X 100 before being incubated for 20 h at 37 ◦C in a zymography development buffer (50 mM Tris-HCl, pH 7.5, containing 200 mM NaCl and 5 mM CaCl2). After destaining and staining zymographic gels with a 0.05% Coomassie Brilliant Blue R-250 solution, zymograms were scanned, and density was calculated by ImageJ software version 1.52.

5.9. Western Blot Analyses of Cardiac Discoidin Domain Tyrosine Kinase Receptor 2 (DDR-2),Citrullinated Histone H3 (H3Cit), Vimentin in (Exp. C)

To determine the molecular mass of DDR-2, citrullinated histone and vimentin SDSPAGE was performed using 10% (w/v) acrylamide gel. The proteins were diluted (to 20 ug) in Laemli sample buffer (Invitrogen-Waltham, MA, USA). Following SDS-PAGE, the proteins were transferred onto a nitrocellulose membrane (Invitrogen Waltham, United States) and blocked in TBS-Tween buffer (20mMTris (pH 7.4–7.6), 0.5MNaCl, 0.05% Tween) with 5% (w/v) milk. The membranes were then incubated overnight in TBST ween and 1% milk in the presence of primary antibody at 4 ◦C. The next day, the membranes were incubated with secondary horseradish peroxidase, and detection was carried out using enhanced chemiluminescence (Amersham Biosciences, Buckinghamshire, UK)

5.10. Determination of Cardiac Myeloperoxidase (MPO) Activity in (Exp. C)

Hexadecyltrimethylammonium bromide (0.5%) was added to the phosphate buffer (pH 6.0) before the heart tissues were homogenized. The homogenized samples were cooled to 37 ◦C in a water bath, and then they were placed in liquid nitrogen. After completing these procedures three times, the samples were centrifuged at 15,000× g for 15 min at 4 ◦C, and the supernatants were gathered. The measurement was carried out using a plate with 96 wells. A total of 280 µL of o-dianisidine diHCL and 12 µL of either the sample or the standard (diluted from peroxidase) were pipetted into the plate. After shaking for 59 s, cardiac MPO activity was measured at 490 nm and expressed as µU/mg protein.

5.11. Protein Content Measurement from heart in (Exp. C)

Using a commercial protein assay kit (Bio-Rad Labs, Hercules, CA, USA), aliquots (20 µL) of the diluted samples were mixed with 980 µL of distilled water, with 300 µL of BCA reagent added to each sample. After mixing and following a 10-min incubation, the samples were assayed spectrophotometrically at 595 nm. The protein level was expressed as ug protein/uL.

5.12. Statistical Analysis

The results are reported as mean ± SEM for per group. For statistical comparisons, due to the normal distribution of all group data, the student's two-tailed t-test was used. p values less than 0.05 were considered significant differences.

6. Results

6.1. Verifying That STZ Injured the Pancreatic Tissue, Not the Liver, at the SIXTH Week in (Exp. A)

Since STZ enters cells through Glucose transporter 2 (GLUT2), which is abundant in the liver and pancreas, it was first necessary to confirm that STZ harmed β cells in the pancreas rather than the liver. Therefore, liver inflammation may draw granulocytes; however, our findings show no discernible liver inflammation based on TNF-α expression measurements (**Figure 12.**)

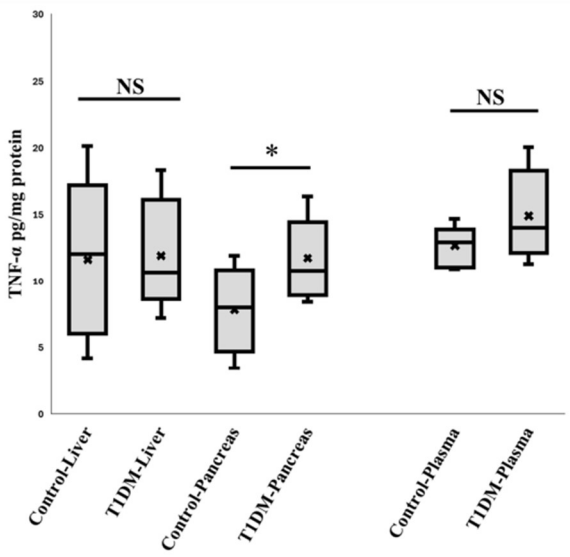

Figure 12. The expression of TNF- α in the plasma, liver, and pancreas. According to the comparison, over the first six weeks, STZ may only damage DNA in the pancreas through GLUT2. Neither the liver nor the other organs were damaged. (n = 10), * $p < 0.05$.

6.2. Validating the Inflammation in Pancreas During the Sixth Week in (Exp. A)

As demonstrated in Table 1, STZ-induced diabetes was associated with a significant decrease in the anti- inflammatory cytokine IL-10 and an increase in the proinflammatory cytokines CXCL-1, IFN-γ, IL-6, IL- 18, and IL-33 [55,70]. (**Table 1.**)

Table 1. Concentration of various inflammatory and anti-inflammatory cytokines in the pancreas. Summary of the analysis of various proinflammatory/anti-inflammatory cytokines in the pancreas of STZ-treated diabetic rats and control. * $p \leq 0.05$, n = 10 (unit: pg/mg protein).

Group	CXCL-1	IFN-γ	IL-6	IL-18	IL-33	IL-10
Control	33.02 ±3.34	21.62 ± 2.44	40.81 ± 5.63	77.67 ± 4.83	708.38 ± 76.19	451.95 ± 152.31 *
STZ	46.85 ± 3.32 *	29.46 ± 2.00 *	55.44 ± 3.29 *	130.75 ± 17.46 *	1027.26 ± 113.47 *	153.71 ± 18.73
Cytokine	inflammatory	inflammatory	inflammatory	inflammatory	inflammatory	anti-inflammatory

6.3. PAD4 mRNA Level in the Pancreas at the Sixth Week in (Exp. A)

PAD4 is implicated in NETs and plays a significant role in NETosis. Thus, we investigated the pattern of PAD4 gene expression in pancreatic tissue from STZ-treated and untreated control rats concurrently with the protein level investigations. According to our RT-PCR results, pancreatic samples from treated animals had a noticeably greater PAD4 mRNA level than the controls. ($2^{-\Delta\Delta CT}$: 1.018 ± 0.408 vs. 3.122 ± 1.151). Neutrophil infiltration may be explained by the elevated level of PAD4 mRNA, but more research is required to validate this. (**Figure 13.**)

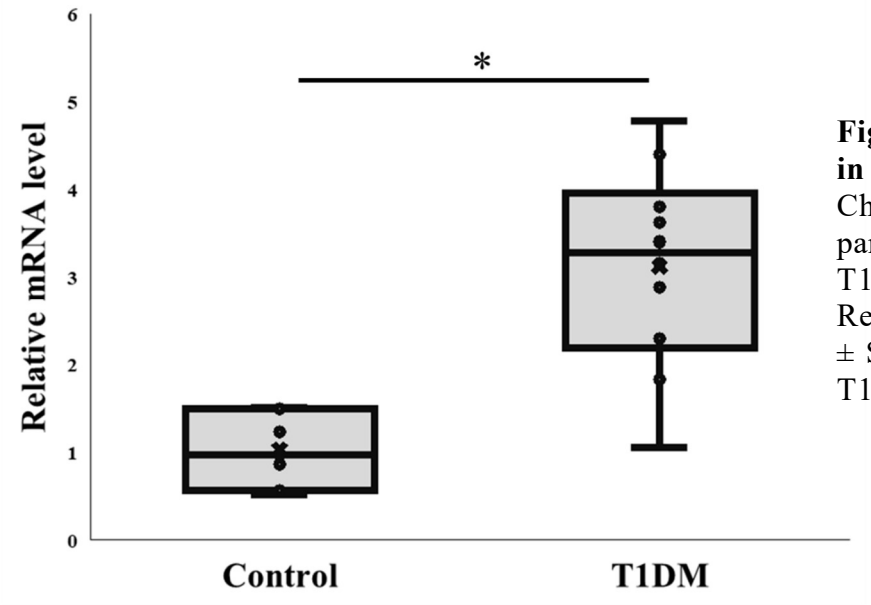

Figure 13. PAD4 mRNA levels in Pancreas.
Change of PAD4 mRNA in pancreas between control and T1DM group. ($P < 0.05$). Results are presented as mean ± S.E.M. (Control, n=7; T1DM, n=10)

6.4. The Expression of PAD4 and Citrullinated Protein in the Pancreas at the Sixth Week in (Exp. A)

Our primary findings on PAD4 are significant enough to meaningfully depict the difference between control and T1DM groups in the pancreas in order to determine NET ($p < 0.05$). Figure 14 shows that the T1DM group has higher levels of expressed PAD4 than the control group, as

determined by quantifying the protein expression and normalizing it to the internal control (beta actin) from extracted pancreas. According to a review paper, PADs in various tissues may play a significant role as a regulator during the pathogenic process of type 1 diabetes. Additionally, we compared the levels of CITH3 in the control and T1DM groups and found that the latter had a considerably higher level of CITH3 than the former. To guarantee the citrullinated substrate for PAD4 and assess the effectiveness of the disease animal model, we assessed the intensity of CITH3 in the pancreas between the control and T1DM groups in the current investigation, which was based on the hypothesis of post-translational modification. (**Figure 14.)**

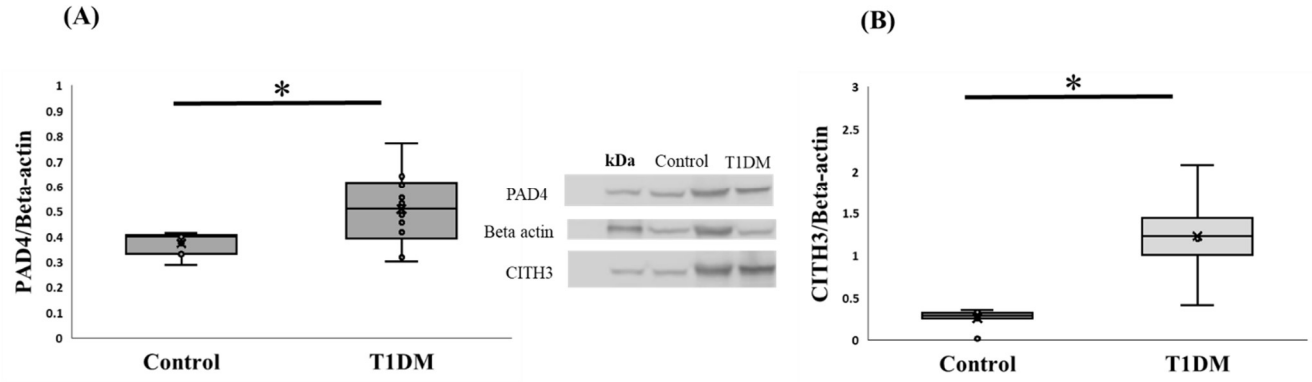

Figure 14. (A) PAD4 protein expression in Pancreas. PAD4 protein level between Control and T1DM against internal control (Beta-actin), elucidating PAD4 expression in T1DM was greater than in Control within pancreas (*P < 0.05). Results arepresented as mean ± S.E.M. (Control, n=7; T1DM, n=10) (B) CITH3 levels in Pancreas. Change of the expression of citrullinated histone-3 (CITH3) between Control and T1DM group. The result indicated successful induction of T1DM according to citrullinated level (*P < 0.05). Results arepresented as mean ± S.E.M. (Control, n=8; T1DM, n=6)

6.5. Ca^{2+}: A Prerequisite Cofactor for Citrullination Among PADs in the Sixth Week in (Exp. A)

Because PAD4 is a calcium-dependent enzyme, when calcium becomes stuck in the active pocket, it starts to citrullinate. Here, we examined the alteration in the pancreatic microenvironment linked to PAD4 expression by measuring Ca^{2+} levels between the control and T1DM groups. According to our findings, PAD4 may bind to calcium ions and boost citrullination activity in T1DM, causing the pancreas to produce less calcium ions than the control group. (**Figure 15.)**

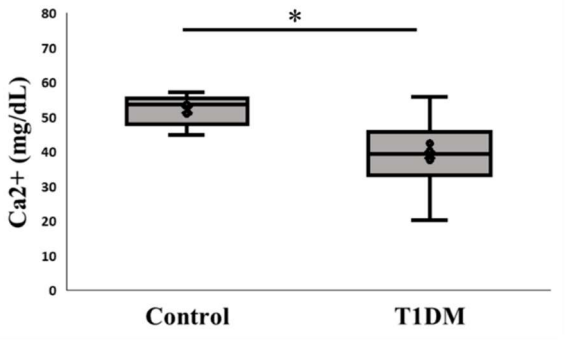

Figure 15. Ca^{2+} content in Pancreas. Change of the expression of Calcium ion between Control and T1DM group, Ca^{2+} is a cofactor for PAD4 and our measurement presented profound impact in pancreas between Control and T1DM group (*P < 0.05). Results are presented as mean ± S.E.M. (Control, n=5; T1DM, n=6)

6.6. Blood Glucose Measurement Before Termination in (Exp. A) and B

In order to accurately determine the state of TDM, the procedure for STZ-induced T1DM induction requires blood glucose to be confirmed prior to sacrifice. In experiments A and B, before termination, we measured the blood glucose levels. Every blood glucose reading between the STZ and control groups was significant. (**Figure 16.**)

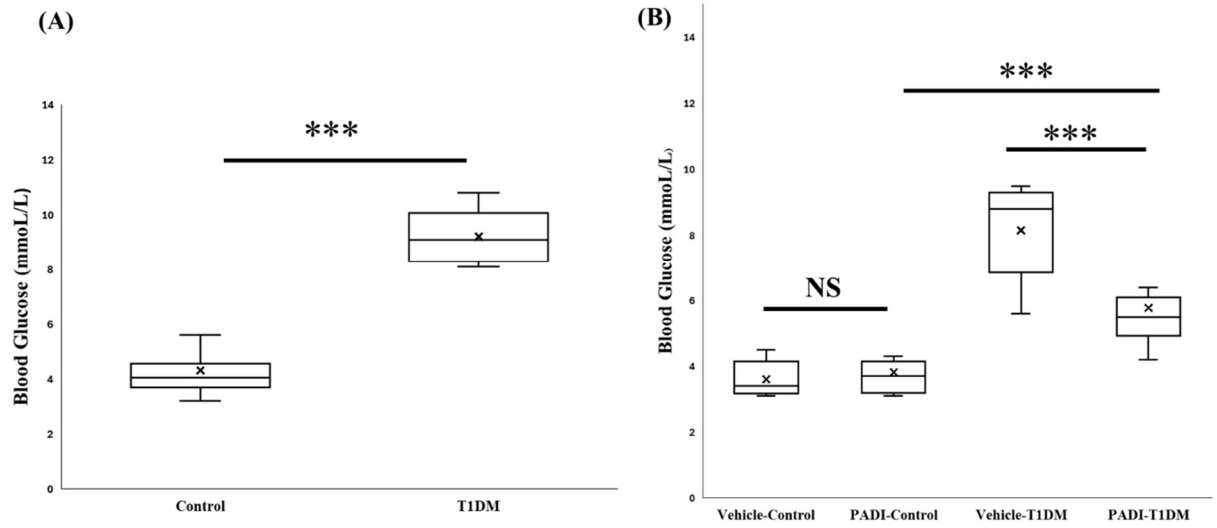

Figure 16. Blood Glucose level before termination (A) At 6th week, by confirming blood glucose levels, T1DM was successfully induced. (B) In experiment B, we used a PADs inhibitor (PADI) to further examine PAD4 expression. After ten days of dosing, we also checked the blood glucose level. ***P < 0.001 (All groups, n=10)

6.7. NETosis Level in the Serum and Pancreas in (Exp. B)

Neutrophil elastase (NE) plays a critical role in extracellular trap formation (NETosis). We looked at NE expression in the pancreas and serum to make sure T1DM was successful in causing NETosis. Despite not being evident in the serum, Cl-amidine suggested a substantial difference between the control and STZ groups. **(Figure 17.)**

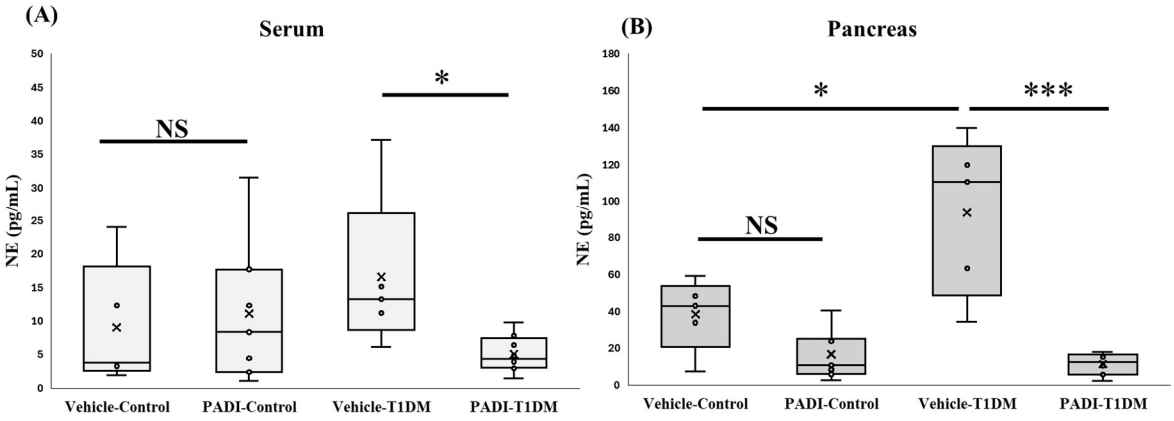

Figure 17. NETosis level in Serum and Pancreas in (Exp. B). A component of extracellular trap formation is neutrophil elastase (NE). We employed Cl-amidine, one of the PADs inhibitors (PADI). *P < 0.05, ***P < 0.001, (A) Vehicle-Control, n=5; PADI-Control, n=7, Vehicle-TIDM, n=5, PADI-T1DM, n=8 (B) Vehicle-Control, n=5; PADI-Control, n=7, Vehicle-TIDM, n=5, PADI-T1DM, n=7

6.8. The Expression of Various Cytokines in the Heart

In this study, cardiac cytokines were measured to map the inflammatory status in the heart. We obtained significant results (IL-6, IL-33, IFN-γ, and TNF-α: $p < 0.05$, IL-18:$p < 0.01$) for primary confirmation. The inflamed status of the heart was determined due to a high level of inflammatory cytokines in the STZ-DM group. Results are presented as mean + SEM, n = 5–9/group. **(Figure 18.)**

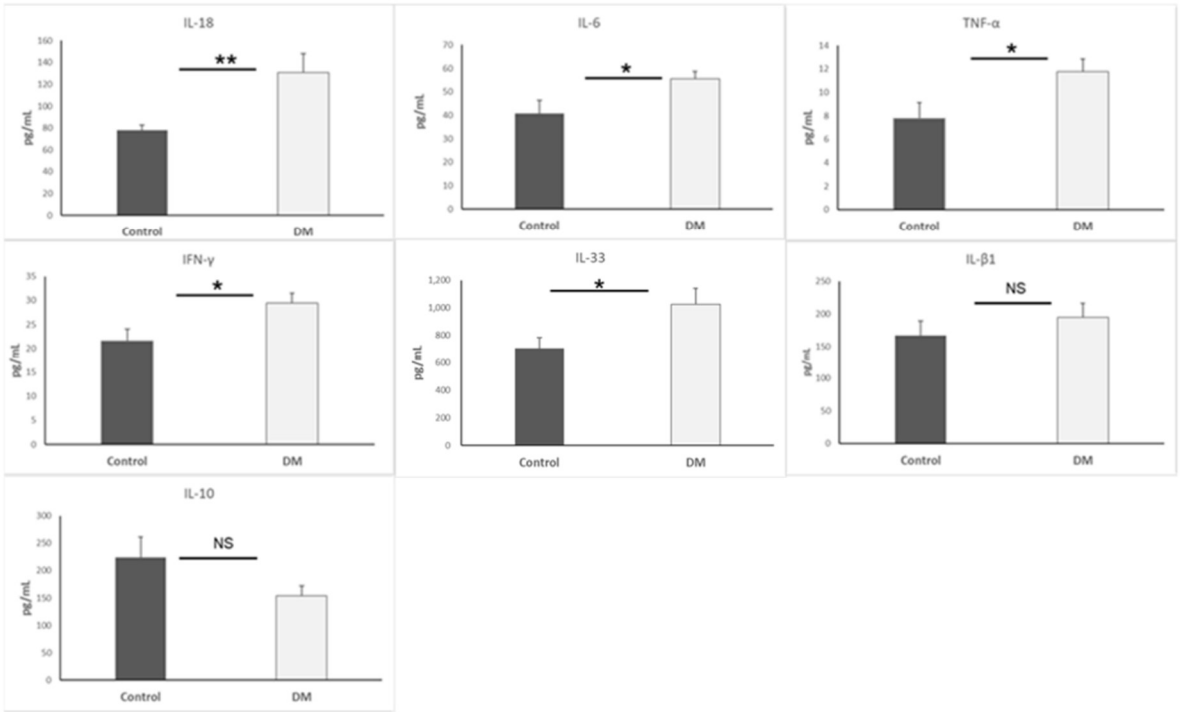

Figure 18. Cytokines Expression in Heart *, p < 0.05; **, p < 0.01; NS, non-significant.

6.9. Basic ROS Examination in the Heart

ROS is one of the main root causes of an EndMT microenvironment. We utilized Peroxynitrite (ONOO−) and MPO to estimate the ROS condition. The data only presented increased peroxynitrite ($p < 0.01$)) in STZ, suggesting a high ROS surrounding in the cardiac area. Results are presented as mean + SEM; n = 4–9/group.(**Figure 19.**)

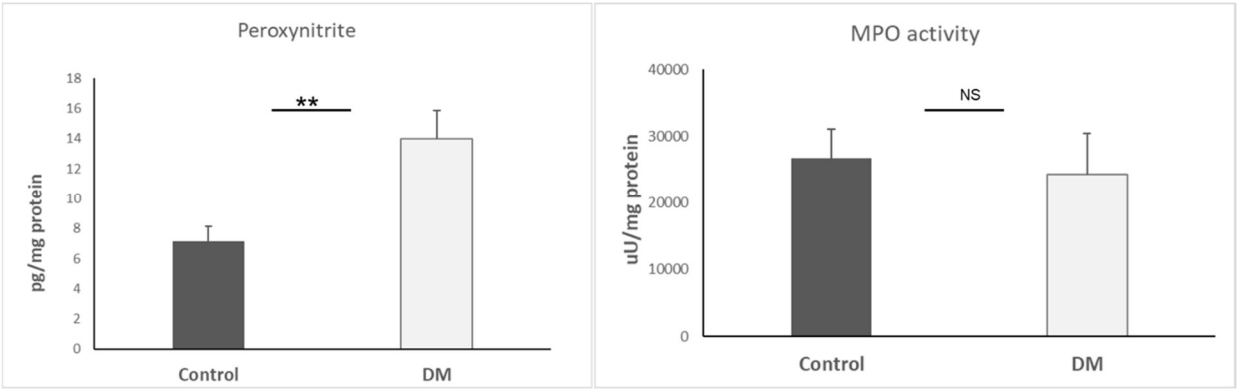

Figure 19. Peroxynitrite and MPO activity Expression in Heart **, $p < 0.01$; NS, non-significant.

6.10. Nitric Oxide Synthases (NOS) Determination in the Heart

Here, we detected inducible NOS (iNOS), endothelial NOS (eNOS), and neuronal ROS (nROS) in cardiac tissue. Our data showed that iNOS was only significantly higher in the STZ-DM group ($p < 0.05$). As a result, immune cells were likely to accumulate in the cardiovascular system. Results are presented as mean + SEM; n = 5–6/group.(**Figure 20.)**

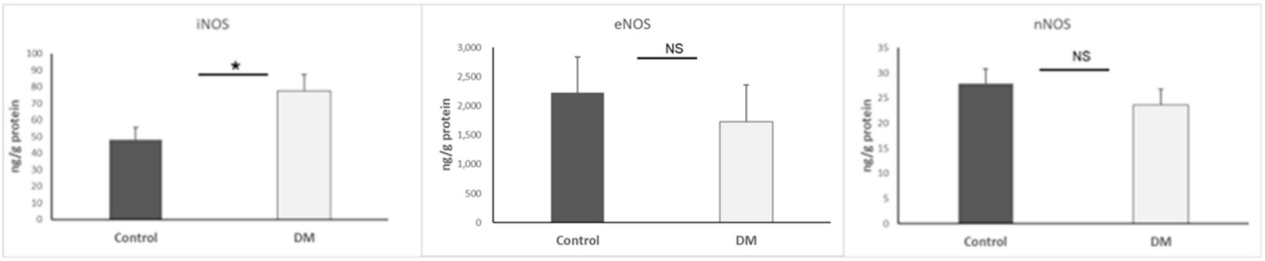

Figure 20. iNOS, eNOS and nMOS Expression in Heart *, $p < 0.05$; NS, non-significant.

6.11. The Assessment of EndMT by DDR-2, MMP-2, and TIMP-1 in the Heart

For the purpose of assessing EndMT, we observed DDR-2, MMP-2 activity, and TIMP-1. The underlying mechanism is that TIMP-1 is capable of inhibiting MMP-2, and DDR-2 can promote MMP-2-mediated proliferation. Interestingly, our data indicated that MMP-2 ($p < 0.001$) and TIMP-1 ($p < 0.01$) were decreased simultaneously in the hearts of the STZ-DM group.

Nevertheless, DDR-2 was increased in the hearts of the STZ-DM group ($p < 0.05$). Results are presented as mean + SEM; n = 5–8/group. (**Figure 21.)**

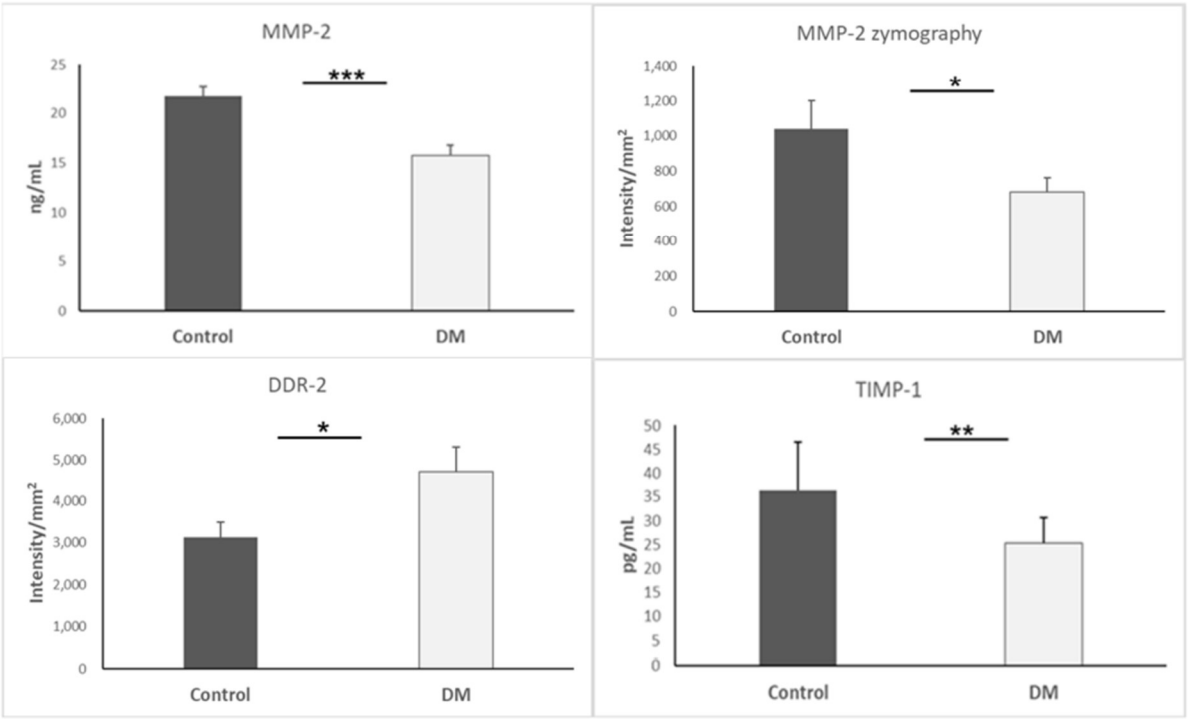

Figure 21. MMP-2, MMP-2 Zymography, DDR-2 and TIMP-1 Expression in Heart *, p < 0.05; **, p < 0.01; *** p < 0.001. MMP-2, Matrix Metalloproteinase-2; DDR-2, Discoidin Domain Receptor 2; TIMP-1, Tissue inhibitor of metalloproteinases

6.12. Biomarkers of Mesenchymal Cells and Neutrophils in the Heart

Continuously, we measured citrullinated histone to confirm whether CXCL1 attracted neutrophils. Additionally, we measured some typical biomarkers (vimentin [71], versican, and α-SMA) to sense mesenchymal cells [72]. Our data indicated that vimentin was lower ($p < 0.01$)but α-SMA was higher ($p < 0.05$) in the STZ-DM group. Additionally, the STZ-DM group presented high CXCL1 ($p < 0.01$) and H3Cit ($p < 0.05$) levels, proving that neutrophils were able to infiltrate the heart during EndMT. Results are presented as mean + SEM; n = 6–15/group.(**Figure 22.**)

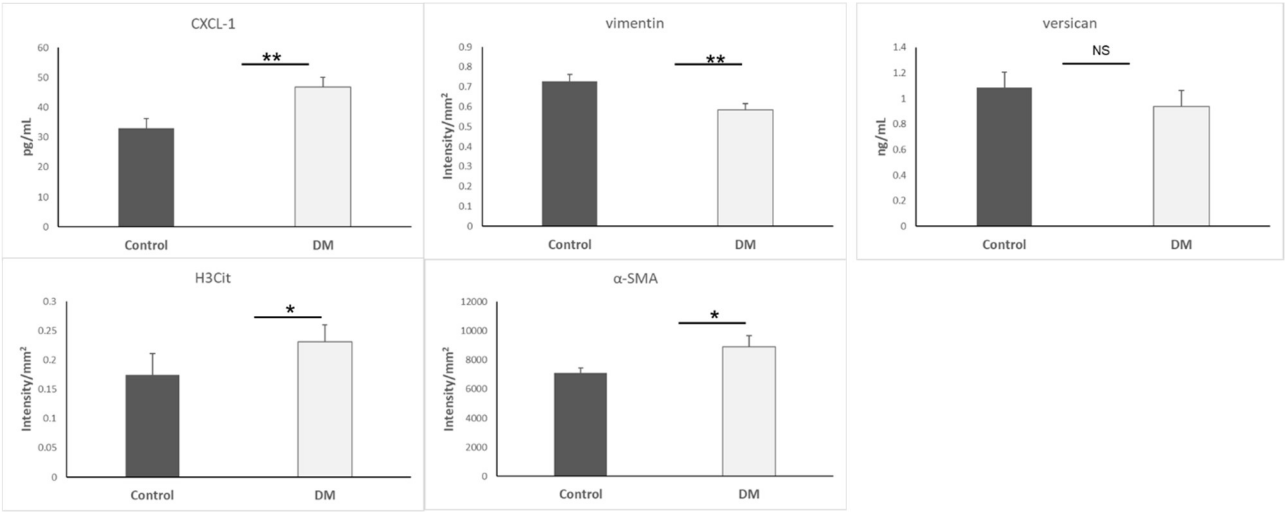

Figure 22. CXCL-1,Vimentin, H3Cit ,α-SMA and versican Expression in Heart *, p < 0.05; **, p < 0.01; NS, non-significant. CXCL-1, C-X-C Motif Chemokine Ligand 1; H3Cit, Histone H3 citrullination; α-SMA, Alpha-Smooth Muscle Actin

6.13. TGF-β Level of Heart, Aorta, and Plasma

TGF-β is an important factor for EndMT and an upstream indicator to trigger EndMT [73]. We continued to detect TGF-β expression since we obtained lower vimentin in the STZ-DM group [74]. The TGF-β level in the heart of the STZ-DM group was exceedingly lower, as proven by statistical significance ($p < 0.0001$), as well as in the aorta ($p < 0.05$) and plasma ($p < 0.05$). Results are presented as mean + SEM; n = 4–8/group.(**Figure 23)**

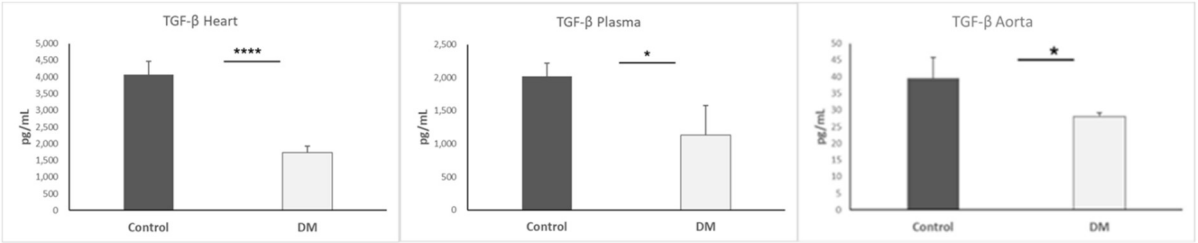

Figure 23. TGF-β Expression in Heart, Plasma and Aorta. *, p < 0.05; **** p < 0.0001.

6.14. Endothelin-1 Expression in Heart and Aorta

Endothelin-1 has been linked to the pathophysiology of other biological diseases, especially irregular EndMT [75]. We also measured endothelin-1 expression in the heart and aorta. Our data only indicated that endothelin-1 expression in the aorta of the STZ-DM group was higher than the control group ($p < 0.05$) [76]. Results are presented as mean + SEM; n = 5–7/group. **(Figure 24.)**

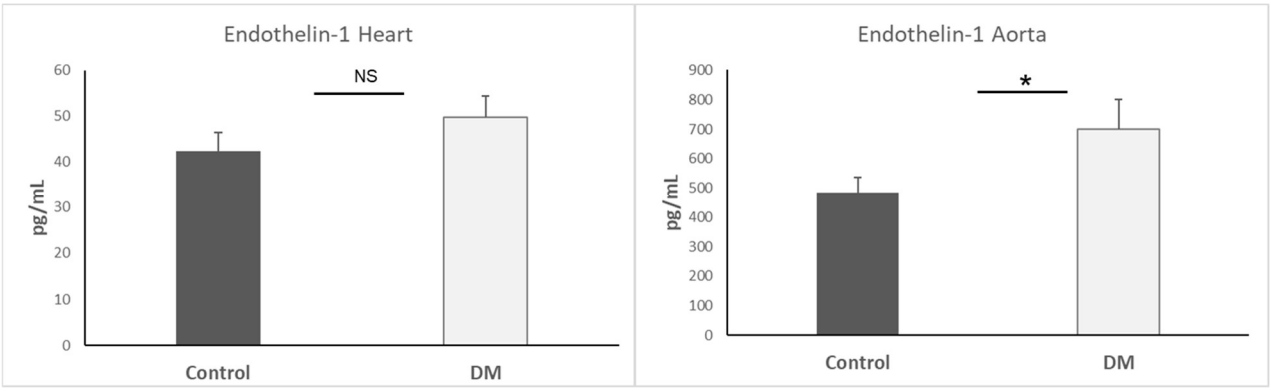

Figure 24. Endothelin-1 Expression in Heart and Aorta *, $p < 0.05$; NS, non-significant.

7 Discussion

In this study, we first established a PAD4 enhancement group to observe overexpression of PAD4 in the STZ-induced pancreas. We then used Cl-amidine to inhibit PAD4 and evaluate systemic inflammation resulting from NETosis. Furthermore, we examined the pancreas-heart axis by assessing cytokines, chemokines, and various EndMT biomarkers in both the heart and aorta. Our findings may offer reasonable insights into the development of diabetic cardiomyopathy.

In the diabetic pancreas, elevated PAD4 expression promotes β-cell destruction through NETosis, while in the diabetic heart, the resulting cytokine storm and oxidative stress contribute to EndMT and cardiac fibrosis. As both processes involve CITH3 and neutrophil activation, we propose that PAD4 activity orchestrates a shared citrullination-driven inflammatory axis linking islet pathology to cardiovascular complications in T1DM. Targeting CITH3 may thus attenuate not only pancreatic autoimmunity but also downstream cardiac remodeling [77].

The role of citrullination and PADs in T1DM has recently gained significant attention. Most previous studies have concentrated on PAD2 and PAD4, particularly elucidating the mechanisms of glucokinase citrullination in the pancreas and liver of NOD mice. In contrast, the present study specifically investigated PAD4 expression and its link with inflammation in an STZ-induced T1DM rat model [78].

Various PTMs, including citrullination, oxidation, phosphorylation, acetylation, methylation, deamidation, and carbonylation, have been implicated in modulating T1DM autoimmunity, glucose regulation, and insulin metabolism. However, whether these PTMs are causative factors or secondary consequences of T1DM pathology remains uncertain. Although animal models and ex vivo studies have provided valuable insights, their findings cannot fully

replicate the complexity of human T1DM. Previous research demonstrated an increase in citrullinated protein levels in STZ-induced T1DM models. However, the specific contribution of PAD4 to disease pathogenesis requires further clarification.

PAD4 is a critical mediator of NETosis, a process exacerbating inflammatory responses. While numerous studies have reported elevated citrullinated protein levels in autoimmune diseases, the direct evaluation of PAD4 protein expression in T1DM remains limited. Our results demonstrate significantly higher PAD4 mRNA and protein levels in the pancreas of T1DM group compared to the controls. This observation aligns with the findings from various immune-mediated conditions, where increased PAD activity correlates with disease severity. Moreover, PAD4 activation is calcium-dependent, and our data reveal decreased pancreatic Ca2+ content in the T1DM group, suggesting calcium mobilization into PAD4′s active site during enzymatic activation [79]. Simultaneously, increased levels of CITH3, a hallmark biomarker of NETosis, were observed, further reinforcing PAD4′s role in disease progression. Recent studies highlighted that PAD4 can initiate NETosis through enhanced ROS production via NADPH oxidase and mitochondrial dysfunction [80]. Although reduced circulating neutrophil numbers have been noted in prediabetes and early T1DM, our findings underscore enhanced local pancreatic NETosis activity rather than systemic changes. Supporting this, the results emphasize that PAD4-driven NETosis substantially contributes to autoimmune disease pathogenesis, including T1DM, and that PAD4 inhibition represents a promising therapeutic strategy [81].

Moreover, while a previous cross-sectional study associated circulating PAD4 gene expression with neutrophil counts in long-term T1DM patients, our findings indicate that pancreatic PAD4 mRNA levels may not directly correlate with neutrophil numbers, suggesting a need for further investigation into localized immune responses. We also analyzed several pro-inflammatory cytokines, including IL-6, IL-18, IL-33, TNF-α, and IFN-γ, which are predominantly secreted by macrophages and T cells during insulitis, leading to β-cell apoptosis and enhanced neutrophil recruitment [82]. Our data corroborate the previous observations, demonstrating increased cytokine levels correlating with β-cell mass reduction. Conversely, the anti-inflammatory cytokine IL-10, which provides protection against β-cell damage, was decreased in T1DM [83], consistent with the earlier findings. Collectively, our data support the hypothesis that PAD4-mediated NETosis contributes significantly to pancreatic inflammation and β-cell destruction in T1DM [84]. The pharmacological inhibition of PAD4 has been shown to attenuate disease progression in animal models. Notably, Cl-amidine, a pan-PAD inhibitor, has demonstrated protective effects against diabetes development in NOD mice by irreversibly

inactivating PAD enzymes. The promising results reported further strengthen the potential for PAD4 inhibitors as therapeutic agents in managing T1DM and other autoimmune diseases [85].

PAD4 expression has been previously implicated in NETosis and β-cell damage in mouse models, but limited data are available on PAD4's role in the pancreas of STZinduced rats [86]. Our findings demonstrate that PAD4 mRNA and protein levels are significantly elevated in diabetic rat pancreas, paralleling the increases in CITH3 and neutrophil elastase activity. Moreover, these effects were mitigated by Cl-amidine treatment, confirming functional inhibition [87]. **(Figure 25.)**

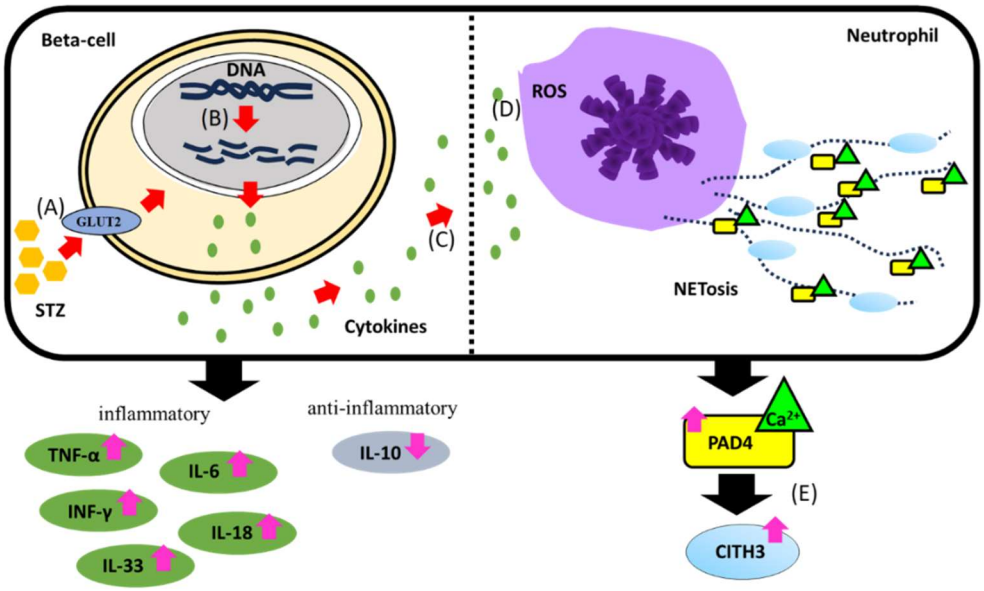

Figure 25. Scheme showing possible mechanism by STZ-induced T1DM

Diabetic cardiomyopathy (DCM) represents a distinct myocardial disorder observed in individuals with diabetes mellitus, characterized by both structural and functional cardiac abnormalities that occur independently of coronary artery disease or hypertension. Clinically, DCM typically manifests as early diastolic dysfunction, which may progress to heart failure with preserved ejection fraction (HFpEF), and in more advanced stages, to heart failure with reduced ejection fraction (HFrEF). Principal pathological features include left ventricular hypertrophy, myocardial fibrosis, and impaired myocardial relaxation, primarily driven by chronic hyperglycemia, insulin resistance, lipotoxicity, oxidative stress, and microvascular dysfunction. Patients are frequently asymptomatic in the early stages, with subtle changes detectable only through advanced imaging techniques such as tissue Doppler or strain imaging. Over time, clinical manifestations including exertional dyspnea, fatigue, and signs of congestive heart failure become apparent. Prognosis remains poor due to limited targeted therapeutic options and the frequent concurrence of other diabetic complications [88]. In this

context, we employed a STZ-induced T1DM rat model to investigate the role of CITH3 in EndMT and the pathogenesis of diabetic cardiomyopathy [89].

Our study of heart EndMT group provides an integrative view of how diabetic conditions promote EndMT and fibrotic remodeling in the heart, highlighting several intersecting molecular pathways. Using the STZ-induced rat model of T1DM, which replicates key human pathological features such as chronic hyperglycemia, systemic inflammation, and cardiac remodeling, we identified a multifaceted interplay among proinflammatory cytokines, oxidative stress, extracellular matrix dysregulation, and epigenetic modifications contributing to endothelial dysfunction and EndMT [90]. These findings offer translational insights relevant to diabetic cardiovascular complications in humans. A central feature of diabetic pathology is the systemic proinflammatory state, which we confirmed by elevated levels of IL-6, IL-18, IL-33, TNF-α, and IFN-γ in cardiac tissue. These cytokines are well-documented contributors to cardiac inflammation and have previously been implicated in diabetic cardiomyopathy [91].

Notably, TNF-α may act upstream to activate CXCL1 signaling, which we found to be upregulated, suggesting a potential biomarker and effector of EndMT [92]. Prior studies have associated CXCL1 and CXCL2 with neutrophil infiltration and myocardial injury in diabetes; our results expand on this by connecting CXCL1 expression to EndMT regulation, a link that remains relatively underexplored [93,94]. Our data also reinforce the pivotal role of oxidative stress in diabetic heart disease. Elevated levels of ROS and iNOS were observed, consistent with prior studies demonstrating ROS-induced endothelial injury. In particular, the accumulation of peroxynitrite ($ONOO^-$) mirrors findings from ischemia-reperfusion models, further implicating oxidative damage in the cardiac remodeling seen in diabetes [95]. This oxidative stress environment appears to disrupt extracellular matrix homeostasis. We observed significantly reduced MMP-2 activity and TIMP-1 expression, aligning with evidence that oxidative stress inhibits MMP function at high ROS levels [96]. These changes are consistent with a profibrotic shift that facilitates EndMT and tissue remodeling. Interestingly, versican—a known ECM proteoglycan and EndMT marker—was not altered in our model, suggesting temporal or disease-stagespecific regulation. An unexpected finding was the reduced TGF-β expression in both the heart and aorta of diabetic rats. While TGF-β is a canonical inducer of EndMT and fibrosis, its downregulation in our model contrasts with reports of increased TGF-β activity in other cardiovascular disease contexts. This suggests a complex, possibly compensatory, regulation of TGF-β signaling in early versus advanced stages of diabetic cardiovascular disease [97]. Supporting this, prior studies show that TGF-β inhibition can

exacerbate aortic wall inflammation in animal models. We also found reduced vimentin content, which may have dual consequences: impairing cytoskeletal integrity and removing its inhibitory effect on ROS synthesis, thereby amplifying oxidative stress [98]. This could also explain the observed increase in CITH3, an epigenetic marker of inflammation linked to NET formation. The relationship between vimentin loss, increased ROS, and CITH3 provides a novel mechanistic insight into how epigenetic and cytoskeletal changes may jointly promote inflammation and EndMT [99].

Further, our study confirms increased expression of α-SMA, a hallmark of mesenchymal transformation. This aligns with in vitro findings of high-glucose-induced EndMT in human endothelial cells and reinforces the relevance of our in vivo results. The upregulation of DDR2—a collagen-binding receptor sensitive to matrix stiffness and hyperglycemia—adds another layer of complexity [100]. DDR2 has recently been implicated in enhancing EndMT in fibrotic environments, and our findings suggest it may act as a mediator between mechanical and metabolic stress in diabetic cardiac remodeling [101]. (**Table 2.**)

Factor/Marker	Change in STZ-DM Model	Role in EndMT/Cardiovascular Pathophysiology
TGF-β	↓	Master EndMT inducer; low levels impair mesenchymal transition
CXCL-1	↑	Chemokine attracting neutrophils; pro-inflammatory
TNF-α	↑	Inflammatory cytokine; upstream activator of CXCL-1
IL-6	↑	Pro-inflammatory; promotes endothelial dysfunction
IL-18	↑	Inflammatory mediator; promotes cytokine storm
IL-33	↑	Involved in innate immunity and inflammation
IFN-γ	↑	Stimulates Th1 responses and immune cell activation
Vimentin	↓	Mesenchymal marker; lower levels suggest impaired transition
α-SMA	↑	Mesenchymal marker: elevation indicates EndMT progression
Versican	≈	ECM proteoglycan; no significant change observed
DDR-2	↑	Collagen receptor; increased in stiff/fibrotic matrix[102,103]
MMP-2	↓	Degrades ECM; decreased activity leads to fibrosis
TIMP-1	↓	Inhibits MMPs; decreased expression disrupts ECM regulation
H3Cit	↑	Histone modification; indicates neutrophil activation and chromatin remodeling
Endothelin-1	↑	Vasoconstrictor; elevated in diabetic aorta, promotes EndMT
Peroxynitrite	↑	ROS indicator; initiates oxidative damage and EndMT
iNOS	↑	Enzyme producing NO; high levels promote inflammation

Table 2. EndMT and cardiovascular markers in diabetic heart. ↑, Higher expression in STZ-DM model; ↓, Lower expression in STZ-DM model; ≈, non-significant between STZ-DM model and control.

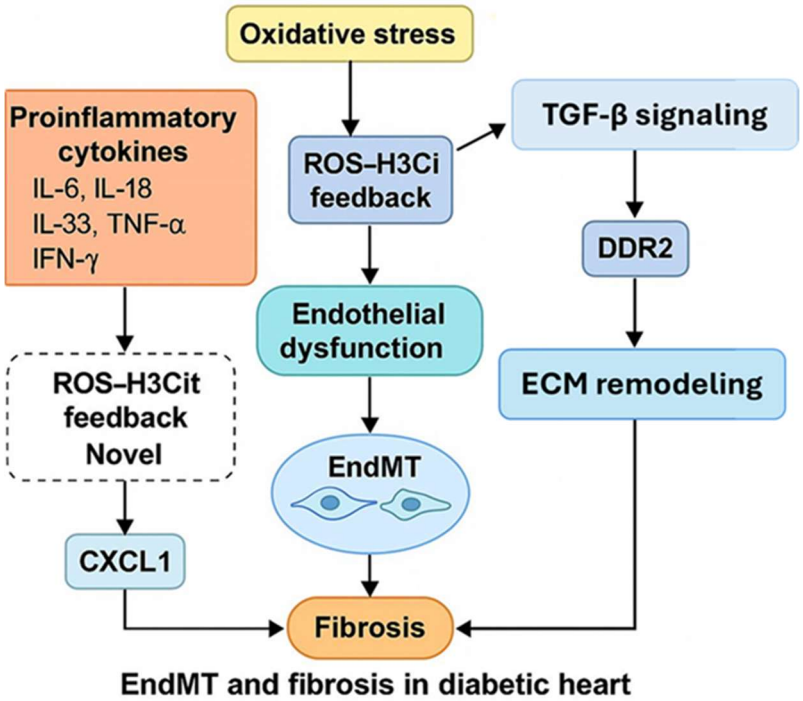

Figure 26. Brief summary of EndMT pathway in the diabetic heart of T1DM. Dotted box, another assumed pathway results in fibrosis.

Our findings of increased CITH3 are particularly significant in this context, as recent studies show histone citrullination is modulated by oxidative stress and linked with NET formation and fibrotic remodeling. Furthermore, confirmation of EndMT markers in human diabetic heart tissues validates the translational relevance of our animal model. (**Figure 26.**) Besides, we propose a model in which hyperglycemia-induced oxidative stress and inflammation initiate endothelial dysfunction, while chemokine signaling, ECM remodeling, and epigenetic changes sustain and amplify this response [104]. The interplay between reduced TGF-β signaling, increased DDR2 expression, and ROS-CITH3 feedback loops is particularly novel and warrants further exploration. By contextualizing these findings within the broader landscape of diabetic cardiovascular research, we highlight new potential targets for early intervention in diabetic cardiomyopathy. (**Figure 27.**)

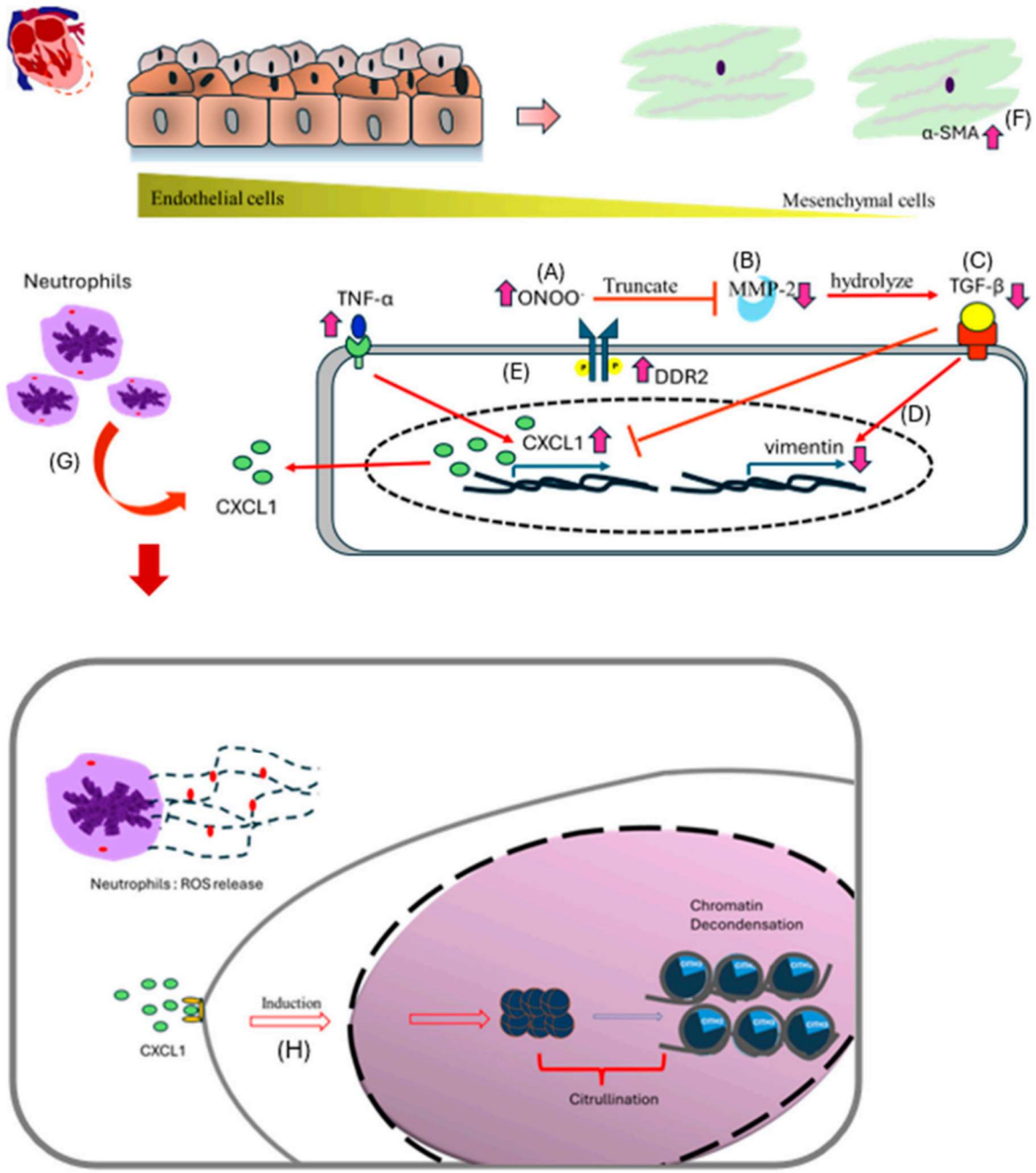

Figure 27. Scheme showing possible EndMT in the heart by STZ-induced T1DM. (**A**) In STZ DM rats, increased peroxynitrite truncates MMP-2, rendering it inactive. (**B**,**C**) MMP-2 facilitates the hydrolysis of TGF-β, causing activated TGF-β to induce the downstream pathway. In STZ DM, decreased MMP-2 suppressed TGF-β transduction [105]. (**D**) Vimentin is one biomarker in mesenchymal cells during EndMT that is activated by TGF-β; a decrease in TGF-β causes a corresponding drop in vimentin [106]. (**E**) On the other side, elevated TNF-α led to an increase in CXCL-1. DDR-2, a different biomarker during EndMT, was aberrantly elevated in the interim. Certain papers about in situ carcinoma suggest that diabetic heart

disease may also have elevated DDR-2 [107]. (**F**) In mesenchymal cells, higher α-SMA is a classical phenomenon during EndMT. (**G**) CXCL-1 from endothelial cells is likely to attract immune cells, particularly neutrophils. In the diabetic heart, neutrophils may close as a result of an inflammatory signal being drawn to them. (**H**) CXCL-1 may induce citrullination in neutrophils [108].

8. Summary

The pancreas-heart axis in T1DM represents a complex interplay between autoimmune, metabolic, and inflammatory processes. The autoimmune destruction of pancreatic β-cells leads to insulin deficiency, which not only disrupts glucose homeostasis but also contributes to systemic inflammation and oxidative stress [83]. These factors adversely affect cardiac function, increasing the risk of diabetic cardiomyopathy and vascular complications. Understanding this axis highlights the importance of integrated therapeutic strategies that address not only glycemic control but also immune modulation and cardiovascular protection in individuals with T1DM.

9. Acknowlegements

I wish to record my profound gratitude to my supervisor, Dr. Krisztina Kupai for their exemplary supervision, scholarly insight, and steadfast support throughout the course of my doctoral studies. Their rigorous critique, constructive guidance, and high standards of academic integrity have been indispensable to the development of this thesis, from its initial conception to its final form.

I am sincerely grateful for the intellectual autonomy provided to me, combined with strategic guidance at pivotal moments. Their mentorship significantly influenced the formulation of research questions, selection of methodologies, and analysis of findings. Furthermore, their encouragement to participate in seminars, collaborations, and conferences substantially broadened the breadth and impact of this work. Beyond their academic advice, I appreciate their patience, generosity of time, and dedication to creating a friendly and collegial research atmosphere within the Department of Oral Biology and Experimental Dental Research. They provided an example of discipline, professionalism, and scientific ethics that will continue to drive my future endeavors.

The research received support from the Incubation Competence Centre of the Centre of Excellence for Interdisciplinary Research, Development and Innovation at the University of Szeged. Prof. Dr. Anikó Pósa, András Szász and Krisztina Kupai are members of the Molecular DiabPharmacology research group. This research was funded by SZTE_SZAOK-KKA_SZAOK-SZBK-2023/5S809 (Kupai K).

10. References

1. Magliano, D.J.; Boyko, E.J.; IDF Diabetes Atlas 10th edition scientific committee *IDF DIABETES ATLAS*; IDF Diabetes Atlas; 10th ed.; International Diabetes Federation: Brussels, 2021; ISBN 978-2-930229-98-0.
2. Banday, M.Z.; Sameer, A.S.; Nissar, S. Pathophysiology of Diabetes: An Overview. *Avicenna J. Med.* **2020**, *10*, 174–188, doi:10.4103/ajm.ajm_53_20.
3. Röder, P.V.; Wu, B.; Liu, Y.; Han, W. Pancreatic Regulation of Glucose Homeostasis. *Exp. Mol. Med.* **2016**, *48*, e219, doi:10.1038/emm.2016.6.
4. Rodrigues Oliveira, S.M.; Rebocho, A.; Ahmadpour, E.; Nissapatorn, V.; De Lourdes Pereira, M. Type 1 Diabetes Mellitus: A Review on Advances and Challenges in Creating Insulin Producing Devices. *Micromachines* **2023**, *14*, 151, doi:10.3390/mi14010151.
5. Xie, Z.; Chang, C.; Zhou, Z. Molecular Mechanisms in Autoimmune Type 1 Diabetes: A Critical Review. *Clin. Rev. Allergy Immunol.* **2014**, *47*, 174–192, doi:10.1007/s12016-014-8422-2.
6. Neefjes, J.; Jongsma, M.L.M.; Paul, P.; Bakke, O. Towards a Systems Understanding of MHC Class I and MHC Class II Antigen Presentation. *Nat. Rev. Immunol.* **2011**, *11*, 823–836, doi:10.1038/nri3084.
7. Marré, M.L.; Piganelli, J.D. Environmental Factors Contribute to β Cell Endoplasmic Reticulum Stress and Neo-Antigen Formation in Type 1 Diabetes. *Front. Endocrinol.* **2017**, *Volume 8-2017*, doi:10.3389/fendo.2017.00262.
8. Han, S.; Donelan, W.; Wang, H.; Reeves, W.; Yang, L.-J. Novel Autoantigens in Type 1 Diabetes. *Am. J. Transl. Res.* **2013**, *5*, 379–392.
9. Yoon, J.-W.; Jun, H.-S. Autoimmune Destruction of Pancreatic β Cells. *Am. J. Ther.* **2005**, *12*, 580–591, doi:10.1097/01.mjt.0000178767.67857.63.
10. György, B.; Tóth, E.; Tarcsa, E.; Falus, A.; Buzás, E.I. Citrullination: A Posttranslational Modification in Health and Disease. *Int. J. Biochem. Cell Biol.* **2006**, *38*, 1662–1677, doi:10.1016/j.biocel.2006.03.008.
11. Ramazi, S.; Zahiri, J. Post-Translational Modifications in Proteins: Resources, Tools and Prediction Methods. *Database* **2021**, *2021*, baab012, doi:10.1093/database/baab012.
12. McLaughlin, R.J.; Spindler, M.P.; Van Lummel, M.; Roep, B.O. Where, How, and When: Positioning Posttranslational Modification Within Type 1 Diabetes Pathogenesis. *Curr. Diab. Rep.* **2016**, *16*, 63, doi:10.1007/s11892-016-0752-4.
13. Mauracher, L. -M.; Posch, F.; Martinod, K.; Grilz, E.; Däullary, T.; Hell, L.; Brostjan, C.; Zielinski, C.; Ay, C.; Wagner, D.D.; et al. Citrullinated Histone H3, a Biomarker of Neutrophil Extracellular Trap Formation, Predicts the Risk of Venous Thromboembolism in Cancer Patients. *J. Thromb. Haemost.* **2018**, *16*, 508–518, doi:10.1111/jth.13951.

14. Guo, G.; Liu, Z.; Yu, J.; You, Y.; Li, M.; Wang, B.; Tang, J.; Han, P.; Wu, J.; Shen, H. Neutrophil Function Conversion Driven by Immune Switchpoint Regulator against Diabetes-Related Biofilm Infections. *Adv. Mater.* **2024**, *36*, 2310320, doi:10.1002/adma.202310320.
15. Wong, S.L.; Demers, M.; Martinod, K.; Gallant, M.; Wang, Y.; Goldfine, A.B.; Kahn, C.R.; Wagner, D.D. Diabetes Primes Neutrophils to Undergo NETosis, Which Impairs Wound Healing. *Nat. Med.* **2015**, *21*, 815–819, doi:10.1038/nm.3887.
16. Yang, M.-L.; Sodré, F.M.C.; Mamula, M.J.; Overbergh, L. Citrullination and PAD Enzyme Biology in Type 1 Diabetes – Regulators of Inflammation, Autoimmunity, and Pathology. *Front. Immunol.* **2021**, *12*.
17. Mikheytseva, I.M.; Amaied, A.; Artiomov, O.V.; Kolomiichuk, S.G.; Kuznetsov, M.K. Relationship between Changes in Retinal Brain-Derived Neurotrophic Factor (BDNF) Concentration and Morphological Changes in Retinal Neurons in Rats with Induced Diabetes and Axial Myopia. *J. Ophthalmol. Ukr. Ž.* **2024**.
18. Junod, A.; Lambert, A.E.; Orci, L.; Pictet, R.; Gonet, A.E.; Renold, A.E. Studies of the Diabetogenic Action of Streptozotocin. *Exp. Biol. Med.* **1967**, *126*, 201–205, doi:10.3181/00379727-126-32401.
19. Kolb-Bachofen, V.; Kolb, H. A Role for Macrophages in the Pathogenesis of Type 1 Diabetes. *Autoimmunity* **1989**, *3*, 145–155, doi:10.3109/08916938909019963.
20. Islam, M.S. Experimental Rodent Models of Type 2 Diabetes: A Review. *Methods Find. Exp. Clin. Pharmacol.* **2009**, *31*, 249–261.
21. Beery, A.K.; Zucker, I. Sex Bias in Neuroscience and Biomedical Research. *Neurosci. Biobehav. Rev.* **2011**, *35*, 565–572.
22. Srinivasan, K.; Ramarao, P. Animal Models in Type 2 Diabetes Research: An Overview. *Indian J. Med. Res.* **2007**, *125*, 451–472.
23. Iannaccone, P.M.; Jacob, H.J. Rats! *Dis. Model. Mech.* 2009, *2*, 206–210.
24. Ghasemi, A.; Jeddi, S.; Kashfi, K. The Laboratory Rat: Age and Body Weight Matter. *EXCLI J.* **2021**, *20*, 1431.
25. Islam, M.S.; Choi, H. Nongenetic Model of Type 2 Diabetes: A Comparative Study. *Pharmacology* **2007**, *79*, 243–249.
26. Sun, B.; Chen, H.; Xue, J.; Li, P.; Fu, X. The Role of GLUT2 in Glucose Metabolism in Multiple Organs and Tissues. *Mol. Biol. Rep.* **2023**, *50*, 6963–6974, doi:10.1007/s11033-023-08535-w.
27. Furman, B.L. Streptozotocin-Induced Diabetic Models in Mice and Rats. *Curr. Protoc.* **2021**, *1*, e78, doi:10.1002/cpz1.78.
28. Long, X.; Yuan, Q.; Tian, R.; Zhang, W.; Liu, L.; Yang, M.; Yuan, X.; Deng, Z.; Li, Q.; Sun, R. Efficient Healing of Diabetic Wounds by MSC-EV-7A Composite Hydrogel via Suppression of Inflammation and Enhancement of Angiogenesis. *Biomater. Sci.* **2024**, *12*, 1750–1760.

29. Zhu, Y.; Xia, X.; He, Q.; Xiao, Q.-A.; Wang, D.; Huang, M.; Zhang, X. Diabetes-Associated Neutrophil NETosis: Pathogenesis and Interventional Target of Diabetic Complications. *Front. Endocrinol.* **2023**, *14*, 1202463, doi:10.3389/fendo.2023.1202463.
30. Kraaij, T.; Tengström, F.C.; Kamerling, S.W.A.; Pusey, C.D.; Scherer, H.U.; Toes, R.E.M.; Rabelink, T.J.; van Kooten, C.; Teng, Y.K.O. A Novel Method for High-Throughput Detection and Quantification of Neutrophil Extracellular Traps Reveals ROS-Independent NET Release with Immune Complexes. *Autoimmun. Rev.* **2016**, *15*, 577–584, doi:10.1016/j.autrev.2016.02.018.
31. Zhu, D.; Song, W.; Jiang, Z.; Zhou, H.; Wang, S. Citrullination: A Modification Important in the Pathogenesis of Autoimmune Diseases. *Clin. Immunol.* **2022**, *245*, 109134, doi:10.1016/j.clim.2022.109134.
32. Kannel, W.B.; Hjortland, M.; Castelli, W.P. Role of Diabetes in Congestive Heart Failure: The Framingham Study. *Am. J. Cardiol.* **1974**, *34*, 29–34, doi:10.1016/0002-9149(74)90089-7.
33. Yu, C.-H.; Suriguga; Gong, M.; Liu, W.-J.; Cui, N.-X.; Wang, Y.; Du, X.; Yi, Z.-C. High Glucose Induced Endothelial to Mesenchymal Transition in Human Umbilical Vein Endothelial Cell. *Exp. Mol. Pathol.* **2017**, *102*, 377–383, doi:10.1016/j.yexmp.2017.03.007.
34. Raffort, J.; Lareyre, F.; Clément, M.; Hassen-Khodja, R.; Chinetti, G.; Mallat, Z. Diabetes and Aortic Aneurysm: Current State of the Art. *Cardiovasc. Res.* **2018**, *114*, 1702–1713, doi:10.1093/cvr/cvy174.
35. Zhang, Z.; Yan, Z.; Yuan, T.; Zhao, X.; Wang, M.; Liu, G.; Gan, L.; Qin, W. PD-1 Inhibition Disrupts Collagen Homeostasis and Aggravates Cardiac Dysfunction through Endothelial-Fibroblast Crosstalk and EndMT. *Front. Pharmacol.* **2025**, *16*, 1549487, doi:10.3389/fphar.2025.1549487.
36. Wang, E.; Chen, S.; Wang, H.; Chen, T.; Chakrabarti, S. Non-Coding RNA-Mediated Endothelial-to-Mesenchymal Transition in Human Diabetic Cardiomyopathy, Potential Regulation by DNA Methylation. *Cardiovasc. Diabetol.* **2023**, *22*, 303, doi:10.1186/s12933-023-02039-4.
37. Yang, S.; Wang, S.; Chen, L.; Wang, Z.; Chen, J.; Ni, Q.; Guo, X.; Zhang, L.; Xue, G. Neutrophil Extracellular Traps Delay Diabetic Wound Healing by Inducing Endothelial-to-Mesenchymal Transition via the Hippo Pathway. *Int. J. Biol. Sci.* **2023**, *19*, 347.
38. Pacher, P.; Szabó, C. Role of Peroxynitrite in the Pathogenesis of Cardiovascular Complications of Diabetes. **2008**.
39. Wilhelmi, T.; Xu, X.; Tan, X.; Hulshoff, M.S.; Maamari, S.; Sossalla, S.; Zeisberg, M.; Zeisberg, E.M. Serelaxin Alleviates Cardiac Fibrosis through Inhibiting Endothelial-to-Mesenchymal Transition via RXFP1. *Theranostics* **2020**, *10*, 3905.
40. Singh, A.; Bhatt, K.S.; Nguyen, H.C.; Frisbee, J.C.; Singh, K.K. Endothelial-to-Mesenchymal Transition in Cardiovascular Pathophysiology. *Int. J. Mol. Sci.* **2024**, *25*, 6180.
41. Tsentidis, C.; Gourgiotis, D.; Kossiva, L.; Marmarinos, A.; Doulgeraki, A.; Karavanaki, K. Sclerostin Distribution in Children and Adolescents with Type 1 Diabetes Mellitus and Correlation

with Bone Metabolism and Bone Mineral Density: Sclerostin in T1DM Children and Adolescents. *Pediatr. Diabetes* **2016**, *17*, 289–299, doi:10.1111/pedi.12288.

42. Prado, A.F.; Batista, R.I.M.; Tanus-Santos, J.E.; Gerlach, R.F. Matrix Metalloproteinases and Arterial Hypertension: Role of Oxidative Stress and Nitric Oxide in Vascular Functional and Structural Alterations. *Biomolecules* **2021**, *11*, 585, doi:10.3390/biom11040585.
43. Bassiouni, W.; Ali, M.A.M.; Schulz, R. Multifunctional Intracellular Matrix Metalloproteinases: Implications in Disease. *FEBS J.* **2021**, *288*, 7162–7182, doi:10.1111/febs.15701.
44. Egea, V.; Zahler, S.; Rieth, N.; Neth, P.; Popp, T.; Kehe, K.; Jochum, M.; Ries, C. Tissue Inhibitor of Metalloproteinase-1 (TIMP-1) Regulates Mesenchymal Stem Cells through Let-7f microRNA and Wnt/β-Catenin Signaling. *Proc. Natl. Acad. Sci.* **2012**, *109*, doi:10.1073/pnas.1115083109.
45. Tyagi Blood Flow Interplays with Elastin: Collagen and MMP: TIMP Ratios to Maintain Healthy Vascular Structure and Function. *Vasc. Health Risk Manag.* **2010**, 215, doi:10.2147/VHRM.S9472.
46. Bellafiore, M.; Battaglia, G.; Bianco, A.; Farina, F.; Palma, A.; Paoli, A. The Involvement of MMP-2 and MMP-9 in Heart Exercise-Related Angiogenesis. *J. Transl. Med.* **2013**, *11*, 283, doi:10.1186/1479-5876-11-283.
47. Ritchie, R.H.; Abel, E.D. Basic Mechanisms of Diabetic Heart Disease. *Circ. Res.* **2020**, *126*, 1501–1525, doi:10.1161/CIRCRESAHA.120.315913.
48. Wu, M.; Li, T.; Li, G.; Niu, B.; Wu, T.; Yan, L.; Wang, S.; He, S.; Huang, C.; Tong, W. LncRNA DANCR Deficiency Promotes High Glucose-Induced Endothelial to Mesenchymal Transition in Cardiac Microvascular Cells via the FoxO1/DDAH1/ADMA Signaling Pathway. *Eur. J. Pharmacol.* **2023**, *950*, 175732.
49. Khan, A.W.; Jandeleit-Dahm, K.A. Atherosclerosis in Diabetes Mellitus: Novel Mechanisms and Mechanism-Based Therapeutic Approaches. *Nat. Rev. Cardiol.* **2025**, 1–15.
50. Takahashi, K.; Ohara, M.; Sasai, T.; Homma, H.; Nagasawa, K.; Takahashi, T.; Yamashina, M.; Ishii, M.; Fujiwara, F.; Kajiwara, T.; et al. Serum CXCL1 Concentrations Are Elevated in Type 1 Diabetes Mellitus, Possibly Reflecting Activity of Anti-Islet Autoimmune Activity. *Diabetes Metab. Res. Rev.* **2011**, *27*, 830–833, doi:10.1002/dmrr.1257.
51. Lo, H.; Lai, T.; Li, C.; Wu, W. TNF-α Induces CXCL1 Chemokine Expression and Release in Human Vascular Endothelial Cells in Vitro via Two Distinct Signaling Pathways. *Acta Pharmacol. Sin.* **2014**, *35*, 339–350, doi:10.1038/aps.2013.182.
52. Testai, L.; Brancaleone, V.; Flori, L.; Montanaro, R.; Calderone, V. Modulation of EndMT by Hydrogen Sulfide in the Prevention of Cardiovascular Fibrosis. *Antioxidants* **2021**, *10*, 910.
53. Chrysanthopoulou, A.; Mitroulis, I.; Apostolidou, E.; Arelaki, S.; Mikroulis, D.; Konstantinidis, T.; Sivridis, E.; Koffa, M.; Giatromanolaki, A.; Boumpas, D.T.; et al. Neutrophil Extracellular Traps Promote Differentiation and Function of Fibroblasts. *J. Pathol.* **2014**, *233*, 294–307, doi:10.1002/path.4359.

54. Delgado-Valero, B.; de la Fuente-Chávez, L.; Romero-Miranda, A.; Visitación Bartolomé, M.; Ramchandani, B.; Islas, F.; Luaces, M.; Cachofeiro, V.; Martínez-Martínez, E. Role of Endoplasmic Reticulum Stress in Renal Damage after Myocardial Infarction. *Clin. Sci.* **2021**, *135*, 143–159, doi:10.1042/CS20201137.
55. Heinrich, P.C.; Behrmann, I.; Haan, S.; Hermanns, H.M.; Müller-Newen, G.; Schaper, F. Principles of Interleukin (IL)-6-Type Cytokine Signalling and Its Regulation. *Biochem. J.* **2003**, *374*, 1–20.
56. Ciesielski, O.; Biesiekierska, M.; Panthu, B.; Soszyński, M.; Pirola, L.; Balcerczyk, A. Citrullination in the Pathology of Inflammatory and Autoimmune Disorders: Recent Advances and Future Perspectives. *Cell. Mol. Life Sci.* **2022**, *79*, 94, doi:10.1007/s00018-022-04126-3.
57. Altamura, S.; Lombardi, F.; Palumbo, P.; Cinque, B.; Ferri, C.; Del Pinto, R.; Pietropaoli, D. The Evolving Role of Neutrophils and Neutrophil Extracellular Traps (NETs) in Obesity and Related Diseases: Recent Insights and Advances. *Int. J. Mol. Sci.* **2024**, *25*, 13633.
58. Karakasis, P.; Theofilis, P.; Patoulias, D.; Vlachakis, P.K.; Antoniadis, A.P.; Fragakis, N. Diabetes-Driven Atherosclerosis: Updated Mechanistic Insights and Novel Therapeutic Strategies. *Int. J. Mol. Sci.* **2025**, *26*, 2196.
59. Mondal, S.; Thompson, P.R. Protein Arginine Deiminases (PADs): Biochemistry and Chemical Biology of Protein Citrullination. *Acc. Chem. Res.* **2019**, *52*, 818–832, doi:10.1021/acs.accounts.9b00024.
60. Yerra, V.G.; Advani, A. Histones and Heart Failure in Diabetes. *Cell. Mol. Life Sci.* **2018**, *75*, 3193–3213, doi:10.1007/s00018-018-2857-1.
61. Kadakol, A.; Malek, V.; Goru, S.K.; Pandey, A.; Gaikwad, A.B. Telmisartan and Esculetin Combination Ameliorates Type 2 Diabetic Cardiomyopathy by Reversal of H3, H2A, and H2B Histone Modifications. *Indian J. Pharmacol.* **2017**, *49*, 348–356, doi:10.4103/ijp.IJP_710_16.
62. Zhou, Y.; Chen, B.; Mittereder, N.; Chaerkady, R.; Strain, M.; An, L.-L.; Rahman, S.; Ma, W.; Low, C.P.; Chan, D. Spontaneous Secretion of the Citrullination Enzyme PAD2 and Cell Surface Exposure of PAD4 by Neutrophils. *Front. Immunol.* **2017**, *8*, 1200.
63. Öğüten, P.N.; Öztürk, S.E.; Dikmen, M. The Investigation of Cytotoxic and Apoptotic Activity of Cl-Amidine on the Human U-87 MG Glioma Cell Line. *Medicine (Baltimore)* **2024**, *103*, e37015.
64. Yao, H.; Cao, G.; Liu, Z.; Zhao, Y.; Yan, Z.; Wang, S.; Wang, Y.; Guo, Z.; Wang, Y. Inhibition of Netosis with PAD Inhibitor Attenuates Endotoxin Shock Induced Systemic Inflammation. *Int. J. Mol. Sci.* **2022**, *23*, 13264, doi:10.3390/ijms232113264.
65. Shen, Y.; You, Q.; Wu, Y.; Wu, J. Inhibition of PAD4-Mediated NET Formation by Cl-Amidine Prevents Diabetes Development in Nonobese Diabetic Mice. *Eur. J. Pharmacol.* **2022**, *916*, 174623, doi:10.1016/j.ejphar.2021.174623.
66. Yang, C.; Dong, Z.-Z.; Zhang, J.; Teng, D.; Luo, X.; Li, D.; Zhou, Y. Peptidylarginine Deiminases 4 as a Promising Target in Drug Discovery. *Eur. J. Med. Chem.* **2021**, *226*, 113840.

67. Ghasemi, A.; Jeddi, S. Streptozotocin as a Tool for Induction of Rat Models of Diabetes: A Practical Guide. *EXCLI J. 22Doc274 ISSN 1611-2156* **2023**, doi:10.17179/EXCLI2022-5720.
68. Melo, Z.; Gutierrez-Mercado, Y.K.; Garcia-Martínez, D.; Portilla-de-Buen, E.; Canales-Aguirre, A.A.; Gonzalez-Gonzalez, R.; Franco-Acevedo, A.; Palomino, J.; Echavarria, R. Sex-Dependent Mechanisms Involved in Renal Tolerance to Ischemia-Reperfusion: Role of Inflammation and Histone H3 Citrullination. *Transpl. Immunol.* **2020**, *63*, 101331, doi:10.1016/j.trim.2020.101331.
69. Kupai, K.; Szucs, G.; Cseh, S.; Hajdu, I.; Csonka, C.; Csont, T.; Ferdinandy, P. Matrix Metalloproteinase Activity Assays: Importance of Zymography. *J. Pharmacol. Toxicol. Methods* **2010**, *61*, 205–209, doi:10.1016/j.vascn.2010.02.011.
70. Xiao, J.; Li, J.; Cai, L.; Chakrabarti, S.; Li, X. Cytokines and Diabetes Research. *J. Diabetes Res.* **2014**, *2014*, 1–2, doi:10.1155/2014/920613.
71. Usman, S.; Waseem, N.H.; Nguyen, T.K.N.; Mohsin, S.; Jamal, A.; Teh, M.-T.; Waseem, A. Vimentin Is at the Heart of Epithelial Mesenchymal Transition (EMT) Mediated Metastasis. *Cancers* **2021**, *13*, 4985, doi:10.3390/cancers13194985.
72. Feng, J.; Li, Y.; Li, Y.; Yin, Q.; Li, H.; Li, J.; Zhou, B.; Meng, J.; Lian, H.; Wu, M.; et al. Versican Promotes Cardiomyocyte Proliferation and Cardiac Repair. *Circulation* **2024**, *149*, 1004–1015, doi:10.1161/CIRCULATIONAHA.123.066298.
73. Angelov, S.N.; Hu, J.H.; Wei, H.; Airhart, N.; Shi, M.; Dichek, D.A. TGF-β (Transforming Growth Factor-β) Signaling Protects the Thoracic and Abdominal Aorta From Angiotensin II-Induced Pathology by Distinct Mechanisms. *Arterioscler. Thromb. Vasc. Biol.* **2017**, *37*, 2102–2113, doi:10.1161/ATVBAHA.117.309401.
74. Li, J.; Huynh, P.; Dai, A.; Wu, T.; Tu, Y.; Chow, B.; Kiriazis, H.; Du, X.-J.; Bach, L.A.; Wilkinson-Berka, J.L.; et al. Diabetes Reduces Severity of Aortic Aneurysms Depending on the Presence of Cell Division Autoantigen 1 (CDA1). *Diabetes* **2018**, *67*, 755–768, doi:10.2337/db17-0134.
75. Åstrand, H.; Rydén-Ahlgren, Å.; Sundkvist, G.; Sandgren, T.; Länne, T. Reduced Aortic Wall Stress in Diabetes Mellitus. *Eur. J. Vasc. Endovasc. Surg.* **2007**, *33*, 592–598, doi:10.1016/j.ejvs.2006.11.011.
76. Beghetti, M.; Black, S.M.; Fineman, J.R. Endothelin-1 in Congenital Heart Disease. *Pediatr. Res.* **2005**, *57*, 16R-20R, doi:10.1203/01.PDR.0000160447.83332.13.
77. Sharma, C.; Hamza, A.; Boyle, E.; Donu, D.; Cen, Y. Post-Translational Modifications and Diabetes. *Biomolecules* **2024**, *14*, 310, doi:10.3390/biom14030310.
78. Battaglia, M.; Petrelli, A.; Vecchio, F. Neutrophils and Type 1 Diabetes: Current Knowledge and Suggested Future Directions. *Curr. Opin. Endocrinol. Diabetes Obes.* **2019**, *26*, 201–206, doi:10.1097/MED.0000000000000485.
79. Ramadan, J.W.; Steiner, S.R.; O'Neill, C.M.; Nunemaker, C.S. The Central Role of Calcium in the Effects of Cytokines on Beta-Cell Function: Implications for Type 1 and Type 2 Diabetes. *Cell Calcium* **2011**, *50*, 481–490, doi:10.1016/j.ceca.2011.08.005.

80. Asmat, U.; Abad, K.; Ismail, K. Diabetes Mellitus and Oxidative Stress—A Concise Review. *Saudi Pharm. J.* **2016**, *24*, 547–553, doi:10.1016/j.jsps.2015.03.013.
81. Bennici, G.; Almahasheer, H.; Alghrably, M.; Valensin, D.; Kola, A.; Kokotidou, C.; Lachowicz, J.; Jaremko, M. Mitigating Diabetes Associated with Reactive Oxygen Species (ROS) and Protein Aggregation through Pharmacological Interventions. *RSC Adv.* **2024**, *14*, 17448–17460, doi:10.1039/D4RA02349H.
82. Garley, M.; Jabłońska, E.; Surażyński, A.; Grubczak, K.; Ratajczak-Wrona, W.; Iwaniuk, A.; Dąbrowska, D.; Pałka, J.A.; Moniuszko, M. Original Article Cytokine Network & NETs. *63*.
83. Abacar, K.; Macleod, T.; Direskeneli, H.; McGonagle, D. How Underappreciated Autoinflammatory (Innate Immunity) Mechanisms Dominate Disparate Autoimmune Disorders. *Front. Immunol.* **2024**, *15*, 1439371.
84. Glowacka, E.; Banasik, M.; Lewkowicz, P.; Tchorzewski, H. The Effect of LPS on Neutrophils from Patients with High Risk of Type 1 Diabetes Mellitus in Relation to IL-8, IL-10 and IL-12 Production and Apoptosis *In Vitro*: Polymorphonuclear Neutrophils Apoptosis in DM1. *Scand. J. Immunol.* **2002**, *55*, 210–217, doi:10.1046/j.1365-3083.2002.01046.x.
85. Aukrust, S.G.; Holte, K.B.; Opstad, T.B.; Seljeflot, I.; Berg, T.J.; Helseth, R. NETosis in Long-Term Type 1 Diabetes Mellitus and Its Link to Coronary Artery Disease. *Front. Immunol.* **2022**, *12*, 799539, doi:10.3389/fimmu.2021.799539.
86. Sodré, F.M.C.; Bissenova, S.; Bruggeman, Y.; Tilvawala, R.; Cook, D.P.; Berthault, C.; Mondal, S.; Callebaut, A.; You, S.; Scharfmann, R.; et al. Peptidylarginine Deiminase Inhibition Prevents Diabetes Development in NOD Mice. *Diabetes* **2021**, *70*, 516–528, doi:10.2337/db20-0421.
87. Du, J.; Wang, N.; Sun, H.; Zheng, L.; Qi, X. Cl-Amidine Attenuates Lipopolysaccharide-Induced Inflammation in Human Gingival Fibroblasts via the JNK/MAPK, NF-κB, and Nrf2 Signalling Pathways. *Hum. Cell* **2023**, *36*, 223–233, doi:10.1007/s13577-022-00822-1.
88. Frustaci, A.; Kajstura, J.; Chimenti, C.; Jakoniuk, I.; Leri, A.; Maseri, A.; Nadal-Ginard, B.; Anversa, P. Myocardial Cell Death in Human Diabetes. *Circ. Res.* **2000**, *87*, 1123–1132, doi:10.1161/01.RES.87.12.1123.
89. Rajbhandari, J.; Fernandez, C.J.; Agarwal, M.; Yeap, B.X.Y.; Pappachan, J.M. Diabetic Heart Disease: A Clinical Update. *World J. Diabetes* **2021**, *12*, 383–406, doi:10.4239/wjd.v12.i4.383.
90. Kovacic, J.C.; Dimmeler, S.; Harvey, R.P.; Finkel, T.; Aikawa, E.; Krenning, G.; Baker, A.H. Endothelial to Mesenchymal Transition in Cardiovascular Disease. *J. Am. Coll. Cardiol.* **2019**, *73*, 190–209, doi:10.1016/j.jacc.2018.09.089.
91. Hsu, P.-C.; Huang, J.-C.; Tsai, W.-C.; Hung, W.-W.; Chang, W.-A.; Wu, L.-Y.; Chang, C.-Y.; Tsai, Y.-C.; Hsu, Y.-L. Tumor Necrosis Factor Receptor Superfamily Member 21 Induces Endothelial-Mesenchymal Transition in Coronary Artery Endothelium of Type 2 Diabetes Mellitus. *Biomedicines* **2022**, *10*, 1282.

92. Korbecki, J.; Maruszewska, A.; Bosiacki, M.; Chlubek, D.; Baranowska-Bosiacka, I. The Potential Importance of CXCL1 in the Physiological State and in Noncancer Diseases of the Cardiovascular System, Respiratory System and Skin. *Int. J. Mol. Sci.* **2022**, *24*, 205.
93. Pan, X.; Kaminga, A.C.; Kinra, S.; Wen, S.W.; Liu, H.; Tan, X.; Liu, A. Chemokines in Type 1 Diabetes Mellitus. *Front. Immunol.* **2022**, *12*, 690082, doi:10.3389/fimmu.2021.690082.
94. Guo, L.-Y.; Yang, F.; Peng, L.-J.; Li, Y.-B.; Wang, A.-P. CXCL2, a New Critical Factor and Therapeutic Target for Cardiovascular Diseases. *Clin. Exp. Hypertens.* **2020**, *42*, 428–437, doi:10.1080/10641963.2019.1693585.
95. Lin, K.-T.; Xue, J.-Y.; Sun, F.F.; Wong, P.Y.-K. Reactive Oxygen Species Participate in Peroxynitrite-Induced Apoptosis in HL-60 Cells. *Biochem. Biophys. Res. Commun.* **1997**, *230*, 115–119, doi:10.1006/bbrc.1996.5897.
96. Hughes, B.G.; Schulz, R. Targeting MMP-2 to Treat Ischemic Heart Injury. *Basic Res. Cardiol.* **2014**, *109*, 424, doi:10.1007/s00395-014-0424-y.
97. Rochmah, N.; Triastuti, I.W.; Deakandi, W.Y.; Irawan, R.; Endaryanto, A. Decreased Serum Transforming Growth Factor- Beta Levels in Indonesian Children with Type 1 Diabetes.
98. Kondo, T.; Takahashi, M.; Yamasaki, G.; Sugimoto, M.; Kuse, A.; Morichika, M.; Nakagawa, K.; Sakurada, M.; Asano, M.; Ueno, Y. Immunohistochemical Analysis of Vimentin Expression in Myocardial Tissue from Autopsy Cases of Ischemic Heart Disease. *Leg. Med.* **2022**, *54*, 102003, doi:10.1016/j.legalmed.2021.102003.
99. Håversen, L.; Sundelin, J.P.; Mardinoglu, A.; Rutberg, M.; Ståhlman, M.; Wilhelmsson, U.; Hultén, L.M.; Pekny, M.; Fogelstrand, P.; Bentzon, J.F.; et al. Vimentin Deficiency in Macrophages Induces Increased Oxidative Stress and Vascular Inflammation but Attenuates Atherosclerosis in Mice. *Sci. Rep.* **2018**, *8*, 16973, doi:10.1038/s41598-018-34659-2.
100. Mihai, C.; Iscru, D.F.; Druhan, L.J.; Elton, T.S.; Agarwal, G. Discoidin Domain Receptor 2 Inhibits Fibrillogenesis of Collagen Type 1. *J. Mol. Biol.* **2006**, *361*, 864–876, doi:10.1016/j.jmb.2006.06.067.
101. Wang, E.; Wang, H.; Chakrabarti, S. Endothelial-to-Mesenchymal Transition: An Underappreciated Mediator of Diabetic Complications. *Front. Endocrinol.* **2023**, *14*, 1050540, doi:10.3389/fendo.2023.1050540.
102. Kim, D.; You, E.; Jeong, J.; Ko, P.; Kim, J.-W.; Rhee, S. DDR2 Controls the Epithelial-Mesenchymal-Transition-Related Gene Expression via c-Myb Acetylation upon Matrix Stiffening. *Sci. Rep.* **2017**, *7*, 6847, doi:10.1038/s41598-017-07126-7.
103. Mitchell, A.V.; Wu, J.; Meng, F.; Dong, L.; Block, C.J.; Song, W.; Zhang, B.; Li, J.; Wu, G. DDR2 Coordinates EMT and Metabolic Reprogramming as a Shared Effector of FOXQ1 and SNAI1. *Cancer Res. Commun.* **2022**, *2*, 1388–1403, doi:10.1158/2767-9764.CRC-22-0013.
104. Bai, P.; Lyu, L.; Yu, T.; Zuo, C.; Fu, J.; He, Y.; Wan, Q.; Wan, N.; Jia, D.; Lyu, A. Macrophage-Derived Legumain Promotes Pulmonary Hypertension by Activating the MMP (Matrix

Metalloproteinase)-2/TGF (Transforming Growth Factor)-B1 Signaling. *Arterioscler. Thromb. Vasc. Biol.* **2019**, *39*, doi:10.1161/ATVBAHA.118.312254.

105. Viappiani, S.; Nicolescu, A.C.; Holt, A.; Sawicki, G.; Crawford, B.D.; León, H.; Van Mulligen, T.; Schulz, R. Activation and Modulation of 72kDa Matrix Metalloproteinase-2 by Peroxynitrite and Glutathione. *Biochem. Pharmacol.* **2009**, *77*, 826–834, doi:10.1016/j.bcp.2008.11.004.
106. Ostrowska-Podhorodecka, Z.; Ding, I.; Norouzi, M.; McCulloch, C.A. Impact of Vimentin on Regulation of Cell Signaling and Matrix Remodeling. *Front. Cell Dev. Biol.* **2022**, *10*, 869069, doi:10.3389/fcell.2022.869069.
107. Goldsmith, E.C.; Zhang, X.; Watson, J.; Hastings, J.; Potts, J.D. The Collagen Receptor DDR2 Is Expressed During Early Cardiac Development. *Anat. Rec.* **2010**, *293*, 762–769, doi:10.1002/ar.20922.
108. Monickaraj, F.; Acosta, G.; Cabrera, A.P.; Das, A. Transcriptomic Profiling Reveals Chemokine CXCL1 as a Mediator for Neutrophil Recruitment Associated With Blood-Retinal Barrier Alteration in Diabetic Retinopathy. *Diabetes* **2023**, *72*, 781–794, doi:10.2337/db22-0619.